Gamma decay of analog resonances in nuclei of the *fp* shell

Yu. V. Naumov, O. E. Kraft, and B. F. Petrov

Physics Research Institute, A. A. Zhdanov State University, Leningrad

I. V. Sizov and S. S. Parzhitskiĭ

Joint Institute for Nuclear Research, Dubna

Fiz. Elem. Chastits. At. Yadra 9, 1282–1349 (November–December 1978)

The results are presented of an experimental investigation of the γ-decay of $p_{1/2}$,$p_{3/2}$, and $f_{5/2}$ analog resonances in ^{59,61,63,65}Cu. The decay schemes of the resonances were constructed, the angular distributions of the γ rays were measured, and the absolute partial γ widths were determined. Data are deduced on the intensities of analog–antianalog transitions, the intensities of β and γ analog transitions, and the positions of states of the core polarization type. The results are given of calculations of the strength functions of the M1 γ-transitions from analogs, and a comparison with the experiment is made.

PACS numbers: 24.30.Eb, 23.20.En, 27.50. + e

INTRODUCTION

A stormy development in the field of nuclear physics associated with isospin was initiated by Anderson's discovery[1] in 1961 of analog states in nuclei of medium atomic mass. It became clear that the concept of isospin can also be used to describe heavy nuclei. Even greater interest was stimulated by Fox's discovery[2] in 1964 of analog states as resonances in the compound nucleus. In nuclear physics, a phenomenon had been discovered with the characteristic features of the so-called microgiant resonance or intermediate structure. Methods of studying analog resonances and also various questions relating to the role of isobar symmetry in nuclei were considered in the review of Ref. 3.

Study of the γ-decay of analog resonances has proved to be an informative and fruitful field of research in nuclear physics. Besides purely spectroscopic information on low-lying states of nuclei, information can be extracted about various effects due to the nature of the analog states. These effects are considered in detail in Ref. 4.

In our view, the most interesting problems are the following.

1. Comparison of the intensities of β and γ analog transitions.

2. Study of the intensities of analog—antianalog transitions.

3. Investigation of the properties of states of the core polarization type.

4. Study of the γ-decay of the fine-structure components of analog resonances.

5. Investigation of the structure of nonanalog proton resonances.

In the present review, we describe the results of an experimental investigation of these problems obtained by analyzing the γ-decay of analog resonances in Cu isotopes. The measurements of the γ-decay of the analogs in ^{59,61,63,65}Cu were made with the EG-5 electrostatic generator of the Laboratory of Neutron Physics at Dubna.

The main aim of the investigation was to study the properties of states of the core polarization type—collective charge-exchange excitations that were detected experimentally for the first time by Gaarde *et al*. in a study of the γ-decay of the $p_{3/2}$ analog in ^{51}V.

The approach to the study of nuclear structure based on analysis of the various collective degrees of freedom in the nucleus and the investigation of elementary modes of nuclear excitations has proved fruitful for both experimentalists and theoreticians.[6]

From the experimental point of view, the study of the elementary excitation modes makes it possible to formulate more precisely and concretely the aim of the investigation, to choose the process in which the given mode may be manifested fairly reliably, and to choose the nucleus in which the given excitation should be studied.

Until recently, information on elementary modes of nuclear excitations was restricted to single-particle excitations and some low-lying collective states. The theoreticians long ago predicted the existence of highly excited (with energy 10–20 MeV) collective states similar to the well-known $E1$ giant resonance. In phenomenological collective models, these resonances correspond, for example, to shape vibrations of various multipolarities and also to degrees of freedom that include changes in the spin and isospin. Resonances of this kind have become known as multipole, or exotic, resonances. Usually, one considers excitations with isospin $\tau = 0$ or 1 and isospin projection $\mu_\tau = 0$. In other words, the excitations exist in the same nucleus as the ground state on which the given excitation is based. However, one can consider elementary modes with isospin projection $\mu_\tau = \pm 1$ and $\tau = 1$. These excitations are based on a ground state that is a state of a neighboring nucleus. The analog state is a well-known

 0090-4759/78/060502-28$02.80

example of such excitations. From the point of view of the microscopic approach, analogs are collective excitations involving a proton and a neutron hole coupled to give angular momentum 0^+.

The present investigation was devoted to collective charge-exchange excitations ($\mu_\tau = -1$) of a different type in which a proton and neutron hole are coupled to give angular momentum 1^+. The main difficulty in an experimental study of multipole resonances is to find a process in which the given state is manifested more clearly than other states of more complicated nature. Such a process must be described by an operator which ensures coherence for the probabilities of transitions to the investigated collective state. In principle, each multiple resonance can be associated with one or several reactions in which an enhancement of the transition to this resonance can be observed. For analog resonances, charge-exchange reactions of the type (p,n) or Fermi β-transitions constitute such processes. For charge-exchange excitations of the type 1^+, Gamow–Teller β-transitions can be suitable for this purpose, but the energy region accessible by means of β processes is small.

It was found some years ago[5] that the $M1$ γ-decay of analog resonances is a suitable process for revealing charge-exchange excitations of the type 1^+. This circumstance, and also other problems associated with the γ-decay of analogs, stimulated intensive investigations in this direction.

Before the start of our investigations of γ-decay of analogs in the Cu isotopes, data had been obtained[4] on the γ-decay of analogs in the nuclei of the $f_{7/2}$ shell and in Sc and V isotopes.

The choice of the investigated nuclei is determined by their shell structure: nuclei near closed shells or filled levels were studied. This circumstance considerably facilitates the interpretation of the experimental data and the theoretical calculations.

Reliability of the interpretation and the possibility of making comparatively simple theoretical calculations which nevertheless reflect reality were the main requirements in the choice of the actual analog resonances to be studied. Investigations were made of analogs of the most clearly expressed single-particle states having a fairly large (≥ 0.6) spectroscopic factor in transfer reactions involving one nucleon (neutron). The choice of odd nuclei has a number of advantages from the experimental point of view (the use of targets with zero spin, convenient energy relations, reliable identification of states) and does not significantly complicate the picture from the theoretical point of view.

1. BASIC NOTIONS ABOUT THE GAMMA DECAY OF ANALOGS

For the decay of analog resonances, $\Delta T = 1$, and therefore only the isovector part of the γ-transition operator contributes to the transition. The information obtained from transitions between low-lying states with $\Delta T = 0$ (the latter are particularly sensitive to the isoscalar part). It is to be hoped that the γ-decay of isobar analog resonances will yield information about the parts of the wave functions that are sensitive to the isovector part of the operator of the electromagnetic transition.

The splitting of this operator into isovector and isoscalar parts determines the main isospin selection rule for γ-transitions: γ-transitions of any multipolarity must satisfy the condition $\Delta T = 0, \pm 1$.

Data on the γ-decay of analogs can be used as a test for the wave functions of low-lying states. It is important that in calculations of transition probabilities from an analog there is no need to write out the wave function of the analog explicitly. It is sufficient to know the wave function $\Psi^{PS}_{T_0+1,\,T_0+1}$ of the parent state and the wave function $\Psi^{f}_{T_0,T_0}$ of the final state.

In the majority of cases, one studies analogs of low-lying states whose wave functions are fairly well known. One can then compare the experiment with the results of calculations made with any model functions

$$\Psi^{f}_{T_0,\,T_0}.$$

On the other hand, if Ψ^f is well known, then data on the γ-decay can give information about the function

$$\Psi^{PS}_{T_0+1,\,T_0+1}.$$

There is a fundamental relation connecting the probability of a γ-transition from an analog state to any level and the ft value for the β-transition from the parent state to the same level. This relation is based on the similarity of the isovector part of the operator of a γ-transition of definite multipolarity and the operator of the β-transition of corresponding type. The relation has been frequently used to analyze transitions in light nuclei.

The most frequent practice is to use the connection between the reduced probability of $M1$ transition from the analog state and the value of the corresponding Gamow–Teller β-transition:

$$ft = 11530/T_0 B(M1,\,\sigma).$$

Here, T_0 is the isospin of the analog and $B(M1,\sigma)$ is expressed in units of $\mu_0^2 = [e\hbar/(2Mc)]^2$.

Gamma-transitions from an analog with isospin T_0 to low-lying states of the nucleus with isospin $T_0 - 1$ and the corresponding β-transitions are usually called β and γ analog transitions.

Detailed study of the γ-decay of analogs in medium and heavy nuclei entails a study of collective charge-exchange degrees of freedom. It is known that the Gamow–Teller β-transitions to low-lying states are hindered compared with the single-particle estimate. Allowance for pairing correlations improves the agreement between the theoretical and experimental ft values.[7]

The experimental values of $\log ft$ of Gamow–Teller β-decay are explained by ideas about the Gamow–Teller collective state, which is a coherent superposition of (p,n^{-1}) excitations coupled to give angular momentum 1^+ (see Refs. 8–10). Configurations of the same

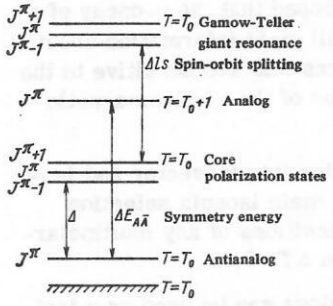

FIG. 1. Energy relationships between analog, antianalog, configuration, and core polarization states.

type are also important for the analysis of the γ-decay of analogs.

Collective charge-exchange excitations appear when allowance is made for residual interactions. The analog state is generated by the isospin—isospin residual interaction and is a superposition of states involving a proton particle and neutron hole coupled to give angular momentum 0^+ (see Refs. 11 and 12). The 1^+ charge-exchange collective excitations appear when the spin–isospin residual interactions are taken into account. To study the γ-decay of analog states, it appears expedient to use basis functions with definite isospin. These functions are constructed in the form of a superposition of particle–hole excitations. The construction of states with definite isospin leads to the appearance of analog, antianalog, and configuration states, states of the core polarization type, and states of the spin-flip type.[13] Figure 1 shows the states that are the most important for the decay of the analogs, and the ground-state configurations of these states. The energy relations between these states are typical of nuclei with $A \sim 50-60$.

In the many-particle shell model, the analog and the antianalog state and the configuration states are determined as follows. Suppose that above a closed inert core with zero isospin and zero spin there is a group of nucleons (an even number) on the level j_1 with total spin $J_0 = 0$ and isospin T_0. We consider only an odd particle on the level j_2. Then the wave function of the analog corresponds to coupling of the odd particle and core with J_0 and T_0 to give total angular momentum $J = j_2$ and isospin $T = T_0 + \frac{1}{2}$. The antianalog state corresponds to the same coupling to give angular momentum $J = j_2$ but isospin $T_0 - \frac{1}{2}$.

All the other states that arise as a result of the recoupling of the spin J_0 and the isospin T_0 are called configuration states in the terminology of Lane. Sometimes, the antianalog state is also included with the configuration states. In what follows, we shall restrict the use of the adjective "configuration" to a smaller class of states, eliminating the antianalog state, the states of the core polarization type, and the spin-flip states.

In the study of the γ-decay of analogs, the most important particle—hole configurations are the ones in which the proton and the neutron hole occupy states in a spin-orbit doublet: $j_n = l \mp \frac{1}{2}$, $j_p = l \pm \frac{1}{2}$. We shall say that states with definite isospin in which such configurations make the main contribution are spin-flip states.

Much attention is devoted to analog–antianalog transitions in investigations into the γ-decay of analogs. Some years ago, when data on the γ-decay of analogs were known for only light nuclei, it seemed that decay by a strong $M1$ transition to the antianalog was the main feature of the γ-decay of analogs. The values of $B(M1)$ for these transitions were found to be a few Weisskopf units. In recent years, data have become available on the decay of analogs in nuclei of the $f_{7/2}$ shell that have necessitated the introduction of new ideas and shown that in the analysis of the γ-decay of analogs it is not possible to restrict oneself to the antianalogs. It was found, first, that there is a large number of analog–antianalog transitions that are strongly hindered compared with the single-particle estimate; second, in many cases the strongest γ-transitions from analogs take place to states situated several MeV above the antianalog; third, analysis of the β and γ analog transitions indicates an important influence of nonsingle particle effects.

The strong hindrance of the analog–antianalog transition is explained by an admixture of core polarization states in the analog. From the theoretical point of view, allowance for states of this type is completely justified, since the probabilities of transitions from the analog to the pure antianalog state and to a pure core polarization state are comparable. From the experimental point of view, the study of core polarization states is a more difficult problem than the investigation of analog–antianalog transitions. These states are situated 1–2 MeV higher than the antianalog. For this region of excitations, the general inadequacy of the spectroscopic data on nuclear levels makes itself felt. In addition, a core polarization state at an appreciable height will be distributed over closely-spaced states, exhibiting a strength-function type phenomenon. Finally, the transition to the study of population of highly excited states entails a considerable increase in the experimental difficulties.

The total decay probability of the analog is distributed between the transitions to the antianalog and the core polarization states. In some nuclei, the transition to the antianalog is predominant. In nuclei of the $f_{7/2}$ shell, in contrast, the transition to the antianalog is hindered and transitions to core polarization states must be clearly manifested. The transition probability does not depend on the state occupied by the odd particle but is determined by the states that are occupied by the excess neutrons. The transitions must be strong if the excess neutrons occupy states with $j_n = l + \frac{1}{2}$ and weak if $j_n = l - \frac{1}{2}$. It should be noted that the residual interactions strongly distort this simple picture, since there occurs an admixture of the antianalog state and the spin-flip states.

Considering the problem of the decay of analog resonances, we arrive at the need to study the strength function of the γ-transitions associated with the analog state. The residual interaction has the consequence

that transitions to spin-flip states are enhanced compared with the unperturbed value. There is a redistribution of the strength of the transition from the antianalog state to a core polarization state and from this latter to a spin-flip state. A fairly strongly collectivized state arises, and this carries the main strength of the $M1$ transition from the analog. This is none other than the Gamow–Teller resonance.

The question of the existence of a Gamow–Teller giant resonance is intimately related to the question of the validity of supermultiplet symmetry in medium and heavy nuclei.[14,10]

Experimental Conditions. The γ de-excitation of analogs in Cu isotopes was investigated with the EG-5 electrostatic accelerator of the Laboratory of Neutron Physics at the Joint Institute for Nuclear Research, Dubna. The maximal proton energy was 5 MeV and the energy spread in the beam 1–3 keV.

The investigation of the γ-decay of analog resonances involves the solution of a number of problems that require knowledge of the reduced probabilities of transitions from analogs to the levels of the studied nucleus. To obtain these quantities, it is necessary to identify the analog, measure the excitation function, measure the γ-decay spectrum of the analog, construct the decay scheme of the resonance, determine the absolute γ widths of the transitions, and measure the angular distributions of the γ's.

The approximate position of the analog is determined from the value of the Coulomb energy with allowance for the results on the transfer reactions in which the analog states are identified. The most reliable identification of analog resonances is by means of the proton elastic scattering reaction measured with high resolution. The definitive identification is made on the basis of all known data with allowance for independent determination of the quantum numbers of the resonance as manifested in the $(p\gamma)$ reaction.

The excitation function in the $(p\gamma)$ reaction is measured by means of large NaI(Tl) crystals. The discrimination threshold is set in such a way as to reduce the low-energy background of the γ's without losing essential information about the decay of the analog. In the measurements, we used thin targets (~10–20 μg/cm^2) deposited on a carbon substrate (~20 μg/cm^2).

The γ-decay spectra of the analogs are measured by means of large (16–40 cm^3) GeLi detectors with resolution 6–7 keV for γ's with energy 8–9 MeV. Impurity lines of different energies are used for the energy calibration. In the analysis of the γ spectra, it is necessary to separate the direct γ transitions from the resonance among the other γ lines. This can be done if the analog resonance has a number of fine-structure components. In this case, the direct γ transitions for the different components of the analog will be shifted in energy by amounts ΔE corresponding to the energy spacings between the components, whereas the de-excitation γ's will remain unchanged in all spectra.

The lines observed in the spectrum are fitted into the decay scheme of the analog in the usual manner with allowance for the energy and intensity balance. Population of a level is assumed to be established if one observes not only its population by a direct transition from the resonance but also the de-excitation of the level.

In the majority of cases, the absolute values of the partial γ widths are determined by the "thick" target method. For these measurements, targets in the form of self-supporting foils of thickness 100–500 μg/cm^2 were used.

The angular distributions of the direct γ's make it possible to determine the multipolarity admixtures. In many cases, information can be obtained about the spins of the resonance or the final state.

Thus, the series of measurements just described above briefly makes it possible to obtain a "complete" experiment, i.e., the absolute values of $B(M1)$, $B(E1)$, or $B(E2)$, and these can be compared with the predictions of various models and theoretical approaches.

The choice of the Cu isotopes for the investigations is largely determined by the fact that we go over to a new shell compared with the nuclei from Ca to ^{58}Ni. The first data on the γ-decay of analogs in isotopes of the $f_{7/2}$ shell were obtained in 1969–1970, and rapid accumulation of data then followed. However, data on the decay of analogs in the nuclei of the fp shell hardly existed at all in 1972, when the present work was begun. Despite the increased experimental difficulties, the transition to the new region of nuclei offers hope of obtaining new information, since many effects in the decay of analogs depend strongly on the shell structure of the investigated nuclei.

2. GAMMA DECAY OF ANALOG RESONANCES IN ^{59}Cu

In the parent nucleus ^{59}Ni (28 protons and 31 neutrons) the $f_{7/2}$ shell is closed for protons and neutrons, and three active neutrons fill the $2p_{3/2}$ level in the $2p1f$ shell. The reaction ^{58}Ni$(dp)^{59}$Ni excites with high probability the well-defined single-particle states quantum numbers $p_{3/2}$, $p_{1/2}$, $f_{5/2}$, and $g_{9/2}$. The ^{59}Ni ground state ($3/2^-$), the first excited state (0.339, $5/2^-$), and the second excited state (0.465, $1/2^-$) carry the main strength of the single-particle $p_{3/2}$, $f_{5/2}$, and $p_{1/2}$ states, respectively. The single-particle $g_{9/2}$ state is at a height of 3.06 MeV and has spectroscopic factor 0.47. Analogs of the low lying states of ^{59}Ni were identified[15] in ^{59}Cu in the reaction $(^3$He$,d)$. The identification criteria were the value of the Coulomb energy, l_p, the spin, and the spectroscopic factor.

Figure 2 shows the positions of the analogs in ^{59}Cu and the proton energies at which they are excited in the reaction ^{58}Ni$(p\gamma)^{59}$Cu. The resonances in this reaction have been studied on several occasions. The excitation function in the reaction ^{58}Ni$(p\gamma)^{59}$Cu in the range of proton energies from 0.8 to 1.9 MeV was studied in Refs. 16 and 17. The quantum numbers of the strongest resonances were obtained in Refs. 16–18: the resonances

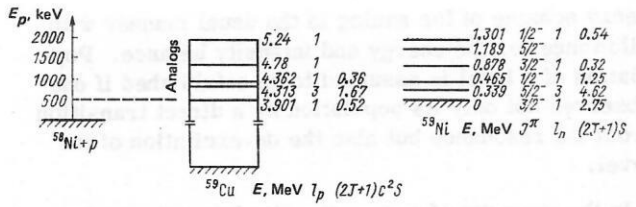

FIG. 2. Scheme of low-lying levels of ^{59}Ni and positions of their analogs in ^{59}Cu.

with $E_p = 1.376$, 1.424, and 1.716 MeV have spin $3/2^-$, and the resonances with $E_p = 1.663$ and $E_p = 1.844$ MeV have spin $1/2^-$. The analog of the second excited state (0.466 MeV, spin $1/2^-$) must be at excitation energy 4.370 MeV. In this region, there is observed a resonance with $E_p = 947$ keV, which has a decay scheme consistent with quantum numbers $1/2^-$. The analog of the first excited state is identified in the reaction (^{3}He,d) at excitation energy 50 keV lower. In this range of proton energies, resonances are not observed in the $(p\gamma)$ reaction. The analog of the state (0.878 MeV, spin $3/2^-$) in the (^{3}He,d) reaction is identified at excitation energy 4.78 MeV. To this excitation energy there corresponds the proton energy $E_p = 1.38$ MeV in the $(p\gamma)$ reaction. In this energy region one can identify two $J^\pi = 3/2^-$ resonances: $E_p = 1.376$ and $E_p = 1.424$ MeV, the second being much stronger. It is not possible to identify unambiguously analogs of the other excited states. In Ref. 19, it is assumed that the resonance with $E_p = 1.833$ MeV is the analog of the ^{59}Ni state at 1.189 MeV. This interpretation encounters serious difficulties because of the large (130 keV) discrepancy in the excitation energy. In addition, it is hard to expect the appearance in the reaction of an analog of the ^{59}Ni state at 1.189 MeV because of the nonstripping nature of this last state. The resonance at $E_p = 1.844$ MeV has the quantum numbers $J^\pi = 1/2^-$ (Ref. 18), and its excitation energy is close to the analog of the excited ^{59}Ni state with energy 1.308 MeV and spin $1/2^-$. However, as will be seen in what follows, the nature of the γ de-excitation of this resonance is not typical for decay of a $p_{1/2}$ analog.

Experimental Conditions. The measurements of the γ-decay of the resonances in ^{59}Cu, as in ^{61,63,65}Cu, were made at the Laboratory of Neutron Physics at Dubna. The protons were accelerated with the electrostatic accelerator EG-5 ($E_{p\,max} = 5$ MeV); the currents were about 10 μA. Self-supporting ^{58}Ni targets (96% enrichment) of thickness 120–140 $\mu g/cm^2$ were used. The yield of γ's from thinner targets would be too low. Since the analogs in ^{59}Cu are at relatively low excitation energies, where the level density is still low, it was not necessary to use very thin targets.

We studied the excitation function in the reaction ^{58}Ni$(p\gamma)^{59}$Cu in the range of proton energies from 800 to 1940 keV. The excitation function was measured by an NaI(Tl) crystal measuring 100×100 mm.

Since the excitation function had been fairly well measured earlier, our main task was to study the γ de-excitation of various resonances and to determine the absolute partial γ widths. We measured the γ-decay spectra of three analog resonances: $E_p = 950$ ($p_{1/2}$ analog), 1424 ($3/2^-$), and 1844 keV ($1/2^-$), and we also studied the decay of two resonances: $E_p = 1883$ and 1923 keV.[20]

Gamma Spectra and Decay Schemes of the Resonances. The γ-decay spectra of the resonances were measured by means of a 40-cm^3 GeLi detector with energy resolution 7–8 keV for γ's with energy ~6.5 MeV. The detector was placed at 90° to the direction of the proton beam. The spectra were measured with a 4000-channel pulse analyzer. In the region up to 2.6 MeV, the energies of the γ's were calibrated by many datum points. At higher excitation energies, convenient datum points were the photopeaks and peaks of single and double γ-transition emission with energy 6.129 MeV in the reaction ^{19}F$(p\alpha)^{16}$O. According to our data, the reaction energy is $Q = 3417 \pm 2$ keV. The decay schemes of the resonances were constructed on the basis of the energy and intensity balance for the observed γ-transitions with allowance for all known data on the ^{59}Cu levels. In Table I, we give the relative intensities of the direct transitions from the resonances to the low-lying ^{59}Cu states. The excitation energies for the corresponding resonances obtained from the analysis of the decay schemes are given in the upper part of Table I.

Absolute Values of the Partial γ Widths. The absolute

TABLE I. Intensities of direct transitions from resonances in ^{59}Cu.

E_{lev}, keV	J^π	$E_p = 950$ keV, $E_{res} = 4349 \pm 5$ keV, $(2J_p+1)\Gamma_p\Gamma_\gamma/\Gamma = 0.096$ eV, $J^\pi = 1/2^-$			$E_p = 1424$ keV, $E_{res} = 4811 \pm 5$ keV, $(2J+1)\Gamma_p\Gamma_\gamma/\Gamma = 2$ eV; $J^\pi = 3/2^-$			$E_p = 1844$ keV, $E_{res} = 5227 \pm 3$ keV, $(2J+1)\Gamma_p\Gamma_\gamma/\Gamma = 3.4$ eV, $J^\pi = 1/2^-$			$E_p = 1883$ keV, $E_{res} = 5267 \pm 3$ keV, $(2J+1)\Gamma_p\Gamma_\gamma/\Gamma = 0.22$ eV, $J^\pi = 3/2$			$E_p = 1923$ keV, $E_{res} = 5311 \pm 4$ keV, $(2J+1)\Gamma_p\Gamma_\gamma/\Gamma = 0.46$ eV		
		I_γ, %	Γ_γ, eV	$B(M1)$, μ_0^2	I_γ, %	Γ_γ, eV	$B(M1)$, μ_0^2	I_γ, %	Γ_γ, eV	$B(M1)$, μ_0^2	I_γ, %	Γ_γ, eV	$B(M1)$, μ_0^2	I_γ, %	$g\Gamma_\gamma$, eV	$gB(M1)$, μ_0^2
0	$3/2^-$	6	0.012	0.012	15	0.08	0.06	90	1.5	0.90	29	0.015	0.01	13	0.03	0.02
491	$1/2^-$	17	0.032	0.04	62	0.32	0.34	5	0.09	0.09	18	0.01	0.008	—	—	—
912	$5/2^-$	—	—	—	—	—	—	—	—	—	7	0.004	0.01	—	—	—
1987	5/2	—	—	—	9	0.045	0.17	—	—	—	—	—	—	—	—	—
2265	3/2	17	0.032	0.32	4	0.02	0.10	4	0.07	0.28	—	—	—	—	—	—
2318	1/2	25	0.048	0.48	—	—	—	—	—	—	8	0.005	0.015	—	—	—
2324	3/2	—	—	—	3	0.015	0.08	—	—	—	—	—	—	57	0.13	0.41
2707	5/2	—	—	—	—	—	—	—	—	—	12	0.007	0.035	—	—	—
2927	5/2	—	—	—	—	—	—	—	—	—	7	0.004	0.025			
3025	(3/2)	11	0.020	0.72	3	0.015	0.22	—	—	—	—	—	—	8	0.018	0.12
3114	(5/2)	9	0.016	0.72	—	—	—	—	—	—	12	0.007	0.06	—	—	—
3130	(3/2)	15	0.028	1.32	—	—	—	—	—	—	—	—	—	7	0.017	0.14
3434	(5/2)	—	—	—	4	0.02	0.65	—	—	—	7	0.004	0.05	—	—	—
3438	(1/2)	—	—	—												
3616	—	—	—	—	—	—	—	—	—	—	—	—	—	6	0.013	0.23
3905	—	—	—	—	—	—	—	—	—	—	—	—	—	9	0.02	0.62

Note. The quantity g is the statistical factor, equal to $(2J_{res}+1)/(2j_p+1)(2J_{targ}+1)$.

values of the partial γ widths were determined by measuring the yield of γ's from a thick target (the energy loss of the proton in the target was much greater than the width of the resonance) at the resonance energy corresponding to the step in the excitation function of the $(p\gamma)$ reaction. We measured the yield of γ's at the proton energy $E_p = 1.844$ MeV, which coincides with the position of the strong resonance with a simple decay scheme. The measurement procedure was as follows. The excitation function of the reaction ^{58}Ni$(p\gamma)^{59}$Cu was measured using a thick (~0.5 mg/cm^2) ^{58}Ni target in the region of proton energies ~1.84 MeV. At the energy corresponding to the step in the excitation function, we measured the spectrum of γ's using an NaI scintillation detector measuring 100×100 mm (the background was taken into account by measuring the γ spectrum to the left of the resonance). At the same proton energies, the γ spectra were measured by means of a GeLi detector. The areas of the photopeaks for all spectra were normalized to the number of incident protons. Since the geometrical sizes and the efficiency for the NaI(Tl) crystals are well known, one can obtain the yield of γ's and calibrate the GeLi detector on the basis of the absolute efficiencies. In this way we obtained the absolute value of the strength $(2J+1)\Gamma_p\Gamma_{\gamma 0}/\Gamma$ for the decay of the resonance with $E_p = 1844$ keV to the ground state; it was found to be 3.0 ± 0.4 eV. Knowing the relative intensities of the γ's for the decay of this resonance, we can obtain the strengths for the other transitions from it. The total strength of the resoance is determined by summing the partial strengths. For the resonance with $E_p = 1844$ keV, the value of $(2J+1) \times \Gamma_p\Gamma_\gamma/\Gamma$ is 3.4 eV with an error of order 20%. Using the absolute calibration of the GeLi detector and knowing the relative intensities of the γ's for the decay of the resonances, we can also obtain the partial and total γ widths for them. Our measured total strengths of the resonances were 1.3 times as large as those of Ref. 17, whereas the relative strengths agreed well with the data of Ref. 17. The method which we used to determine the absolute yields was tested earlier in measurements of the strengths of the resonances in ^{61}Cu and ^{63}Cu (Ref. 21).

To determine the value of Γ_γ from the known strengths of the resonances, it is necessary to know the spins of the resonances. The spins of the resonances at $E_p = 1424$ and 1844 keV are well known: 3/2 and 1/2. The spin of the resonance at $E_p = 950$ keV is apparently 1/2, as follows from the decay scheme of the resonance. The spin of the resonance at $E_p = 1883$ keV was established to be 3/2 in Ref. 19. The spin of the resonance at $E_p = 1923$ keV is also apparently 3/2, which follows from the analysis of the decay scheme of this resonance.

Usually, to determine Γ_γ, one assumes that $\Gamma_p \gg \Gamma_\gamma$. This assumption is justified at proton energies greater than or equal to 1.2 MeV. For the resonance with $E_p = 950$ keV, the ratio $\Gamma_p/\Gamma(\Gamma = \Gamma_p + \Gamma_\gamma)$ determined in Ref. 22 was 1/4. The resulting values of the partial γ widths with allowance for this ratio are given in Table I.

For each resonance in Table I, we have given the $B(M1)$ values in units of μ_0^2. These values were calculated under the assumption of a dipole nature of the γ transitions from the resonances. As a rule, the corrections for possible admixtures of $E2$ transitions are 5–10% for the $B(M1)$ values.[23]

Beta and Gamma Analog Transitions. The ^{59}Cu nucleus undergoes β^+-decay to the levels of the parent nucleus ^{59}Ni. The γ-transitions from the analogs to the ground state of ^{59}Cu and the β^+-transitions from the ground state of ^{59}Cu to the ^{59}Ni parent states are β and γ analog transitions. If we ignore the l part in the operator of the isovector γ-transition, we can obtain a definite relationship between the intensities of the γ and β analog transitions. For the case of ^{59}Cu, this relation has the form (see Eq. (27) in Ref. 4)

$$ft = \frac{11530}{T_0 B(M1, \sigma)} \frac{(2J_i+1)_\beta}{(2J_i+1)_\gamma} = \frac{11530}{T_0 B(M1, \sigma)} \frac{(2J_0+1)}{(2J_A+1)}. \quad (1)$$

In this expression, T_0 is the isospin of the analog, equal to 3/2 for ^{59}Cu; $B(M1, \sigma)$ is the spin part of the γ-transition probability from the analog to the ^{59}Cu ground state expressed in units of μ_0^2; J_0 is the spin of the ^{59}Cu ground state, equal to 3/2; J_A is the spin of the considered analog. Using this formula, one can obtain from the ft value for the β-transition the value of $B(M1, \sigma)$, and this can be compared with the experimental value of $B(M1)$ for the γ-transition between the analog and the ^{59}Cu ground state.

The experimental ft values for the β^+-decay of ^{59}Cu were taken from Ref. 24.

Transitions are observed to many ^{59}Ni states, including the states 0.466 ($1/2^-$), 0.873 ($3/2^-$), and 1.303 MeV ($1/2^-$), whose analogs were studied in the present investigation. The log ft values for transitions to these states are equal to 6.03, 5.31, and 4.70, respectively. The $B(M1, \sigma)$ values were found to be 0.014, 0.038, and $0.32\mu_0^2$. The experimental values of $B(M1)$ for the decays of the corresponding analogs to the ground state are 0.012, 0.06, and $0.90\mu_0^2$. The ratios $B(M1)/B(M1, \sigma)$, which characterize the contribution of the l part to the γ-transition, are equal to 0.8, 1.58, and 2.8. These values agree with the general systematics of the ratio $B(M1)/B(M1, \sigma)$ for the decay of analogs. The contribution of the l part to the γ-transition is comparable with the contribution of the σ part. However, the absence of very large or very small ratios $B(M1)/B(M1, \sigma)$ indicates the presence of correlations between the probabilities of the γ and β analog transitions.

Analog–Antianalog Transitions. The antianalog for the $p_{1/2}$ analog can be only the ^{59}Cu state at 0.491 MeV with quantum numbers $1/2^-$. The spectroscopic factor for this state is not very large (0.55), but the remaining strength of the $p_{1/2}$ state is distributed over many ^{59}Cu levels up to excitation energies of 6 MeV. The experimental value of $B(M1)$ for the $p_{1/2}$ analog–antianalog transition is $0.04\mu_0^2$. The "single-particle" value of $B(M1)$ for this transition, calculated in accordance with Eq. (52) in Ref. 4, is $0.13\mu_0^2$, i.e., the transition is hindered by a factor 3. Allowance for the difference of the spectroscopic factor of the parent state (0.466 MeV, $1/2^-$) in ^{59}Ni (0.62 from 1.00) reduces this dis-

TABLE II. Beta and gamma analog transitions in ^{59}Cu.

E_x^{PS} ^{59}Ni, keV	J^π	lg ft	$B(M1,\sigma)$, μ_0^2	$B(M1)$, μ_0^2	$\frac{B(M1)}{B(M1,\sigma)}$
0	3/2⁻	5.03	0.07	(0.75)	(10)
465	1/2⁻	6.03	0.014	0.012	0.8
878	3/2⁻	5.31	0.038	0.06	1.6
1303	1/2⁻	4.70	0.32	0.90	2.8

Analog–antianalog transitions

State	$B(M1)_{exp}$, μ_0^2	$B(M1)_{theor}$, μ_0^2 (Ref. 4)
$p_{3/2}$	0.75 – 0.07	2.84
$p_{1/2}$	0.04	0.13

crepancy.

The principal strength of the $p_{3/2}$ state in the parent nucleus ^{59}Ni is concentrated in the ground state of this nucleus. As we have noted, the analog of the ^{59}Ni ground state is situated in ^{59}Cu at the height 3.901 MeV. It was difficult to excite this state in the $(p\gamma)$ reaction because of the low energy of the protons ($E_p \approx 500$ keV). We cannot therefore give an experimental value for the analog–antianalog transition probability for $p_{3/2}$ obtained directly from decay of the resonance. However, we can obtain this value in two other ways.

We measured the γ-decay of the resonance with $E_p = 1424$ keV, $3/2^-$, which is the analog of the ^{59}Ni state with energy 0.878 MeV. This state carries a small fraction of the single-particle $p_{3/2}$ strength: its spectroscopic factor is 0.08. If it is assumed that the γ-decay of the analogs is basically determined by the single-particle component of the parent state, it is possible to obtain an estimate of $B(M1)$ for a pure $p_{3/2}$ parent state. The probability of transition from the resonance with $E_p = 1424$ keV to the $3/2^-$ ground state of ^{59}Cu is $B(M1) = 0.06\mu_0^2$. Taking into account the spectroscopic factor of the parent state, we obtain for the reduced probability of the $p_{3/2}$ analog–antianalog transitions in ^{59}Cu the value $B(M1) = 0.75\mu_0^2$.

A different estimate for this quantity can be obtained as follows. As can be seen from Fig. 2, the $p_{3/2}$ analog–antianalog transition is the analog transition with respect to the β-transition from the ground state of ^{59}Cu to the ground state of ^{59}Ni. In this case, we can calculate the value of $B(M1,\sigma)$ in accordance with formula (1) for the γ-transition in which we are interested from the ft value of the corresponding β-decay. The calculations give the value $B(M1,\sigma) = 0.071\mu_0^2$, which is ten times smaller than the $B(M1)$ value obtained above with allowance for the spectroscopic factor of the state at 0.878 MeV ($3/2^-$) in ^{59}Ni. The ratio $B(M1)/B(M1,\sigma) = 10$ does not fit into the systematics of the ratios $B(M1)/B(M1,\sigma)$ for the decay of analogs. Usually, these ratios are in the range 1–5 and are larger in only one or two cases.

From all that we have said, we can only draw the conclusion that for the $p_{3/2}$ analog–antianalog transition $B(M1) \leq 0.75\mu_0^2$, whereas the single-particle estimate is $2.84\mu_0^2$. The data on the intensities of the analog–antianalog transitions in ^{59}Cu and on the intensities of

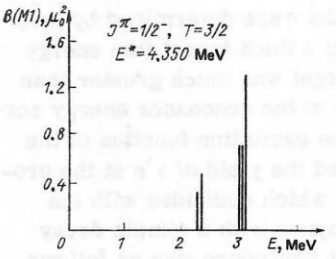

FIG. 3. Values of $B(M1)$ for γ-decay of the $p_{1/2}$ analog in ^{59}Cu (experiment).

the β and γ analog transitions are given in Table II. It can be seen that the obtained values are smaller than the theoretical values.

Core Polarization States. The γ-decay of analogs in ^{59}Cu is characterized by a pronounced selectivity in the population of the low-lying state. In Fig. 3, we show the distribution of the $B(M1)$ values for direct transitions from the $p_{1/2}$ analog with $E_p = 950$ keV. It can be seen that the highly excited ^{59}Cu states are the ones most intensely populated, and that two groups of levels can be distinguished at excitation energies 2.3 and 3.1 MeV. A calculation with allowance for residual interactions (details of the calculations are given in Sec. 5) shows that states with large components of the type $p_{3/2}(p_{3/2}p_{3/2}^{-1})_{+1}$, i.e., states of the core polarization type, must be the closest to the analog states. For reasonable values of the parameters, the excitation energies of the core polarization states agree with the excitation energies of the states that are strongly populated by the decay of the $p_{1/2}$ analog. In Fig. 4 and in Table III we give the results of calculations of the $B(M1)$ distribution of the $p_{1/2}$ and $p_{3/2}$ analogs. It can be seen that the calculations predict the existence of a group of states populated strongly by the γ-decay of the analogs. The calculated value of the sum $B(M1)$ for transitions to core polarization states is $3\mu_0^2$ for the decay of the $p_{1/2}$ analog. The experimental value of the sum $B(M1)$ for transitions to states with excitation energy 2.3 MeV is $0.8\mu_0^2$ and to 3.1 MeV state it is $2.8\mu_0^2$. The following interpretation is the most probable: the core polarization states can be identified with two experimentally observed maxima. The maximum is split into two components because of interactions not taken into account in the calculation.

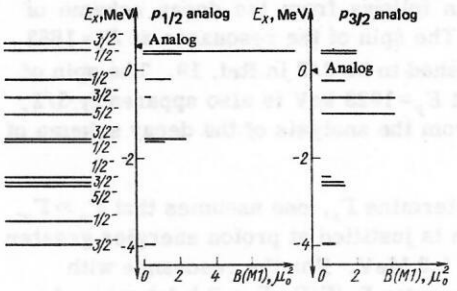

FIG. 4. Values of $B(M1)$ for the γ-decay of the $p_{1/2}$ and $p_{3/2}$ analogs in ^{59}Cu (calculation). The energies E_x are measured from the position of the analog. $G_0 = 1.0$ MeV, $G_1 = 0.7$ MeV, $\Delta = 0.0$, $\varepsilon_{lsp} = 1.0$ MeV.

TABLE III. Wave functions of the states and transition probabilities for $p_{1/2}$ and $p_{3/2}$ analogs in ^{59}Cu.*

J^π	E_x, MeV	$p_{3/2}(p_{3/2}p_{3/2}^{-1})_{1^+}$	$p_{3/2}(p_{1/2}p_{3/2}^{-1})_{1^+}$	$p_{1/2}(p_{3/2}p_{3/2}^{-1})_{1^+}$	$p_{1/2}(p_{1/2}p_{3/2}^{-1})_{1^+}$	$p_{1/2}$ or $p_{3/2}$	$B(M1)$, μ_0^2 $p_{1/2}$	$B(M1)$, μ_0^2 $p_{3/2}$
3/2⁻	0.474	0.197	0.254	0.490	0.715	0.380	8.37	1.93
1/2⁻	0.447	0.352	0.443	0.357	0.535	0.516	1.95	1.90
1/2⁻	−0.193	−0.344	0.474	0.339	0.675	−0.294	1.31	1.26
3/2⁻	−0.610	0.462	0.717	−0.129	−0.433	0.261	0.22	4.31
5/2⁻	−0.980	0.494	0.870	—	—	—	—	4.28
3/2⁻	−1.574	−0.060	−0.168	0.822	−0.534	0.087	2.22	0.009
1/2⁻	−1.602	−0.037	−0.108	0.855	−0.503	0.047	1.12	0.004
1/2⁻	−2.415	−0.681	0.756	0.101	0.025	−0.332	0.004	0.39
3/2⁻	−2.541	0.773	−0.598	−0.102	−0.027	0.182	0.000	1.37
5/2⁻	−2.610	0.870	−0.494	—	—	—	—	1.43
1/2⁻	−3.412	0.647	0.162	0.125	0.062	−0.732	0.001	0.003
3/2⁻	−3.928	−0.382	−0.185	−0.238	−0.125	0.864	0.49	0.83

*$G_0 = 1.0$ MeV, $G_1 = 0.7$ MeV, $\Delta = 0.0$ MeV, $\varepsilon_{lsp} = 1.0$ MeV,. The energies E_x are measured from the analog state.

3. GAMMA DECAY OF ANALOG RESONANCES IN ^{61}Cu

The low-lying states of the parent nucleus ^{61}Ni are well known.[25] The ^{61}Ni ground state (3/2⁻) carries an appreciable fraction of the $p_{3/2}$ strength. The second excited state can be assumed to be a single-particle $p_{1/2}$ state.

The analog state corresponding to the ^{61}Ni ground state must be at excitation energy 6.4 MeV in ^{61}Cu (the difference between the Coulomb energies of ^{61}Cu and ^{61}Ni is 9.41 MeV, the mass difference being 2.23 MeV). The $p_{3/2}$ analog state in ^{61}Cu was identified[26] in the reaction ^{60}Ni(^{3}He, d)^{61}Cu at excitation energy 6.402 MeV. This region of excitation energies is accessible in the $(p\gamma)$ reaction at proton energies of order 1.6 MeV. The excitation function in the reaction ^{60}Ni$(p\gamma)^{61}$Cu was measured[16] in 1957 in the energy range from 725 to 1793 keV. In Refs. 16 and 27, measurements were made of the angular distributions of the strongest γ-transitions for several resonances, and their spins were determined. Naturally, isobar analog resonances were not identified in Refs. 16 or 27. Usually, isobar analog resonances appear in the excitation function of the $(p\gamma)$ reaction as the strongest resonances, this being evidently due to their comparatively simple structure. In the range of excitation energies that we need, four strong resonances with $E_p = 1588$, 1599, 1605, and 1620 keV are observed. In our measurements, the spin value 3/2 for the listed resonances follows from analysis of the decay schemes and the angular distributions of the direct γ-transitions. We assume that these four resonances are fine-structure components of the $p_{3/2}$ resonance, which is the analog of the ^{61}Ni ground state.

The analog of the first excited state of ^{61}Ni (68 keV, 5/2⁻) was identified[26] in the reaction ^{60}Ni(^{3}He, d)^{61}Cu at a height 6.469 MeV. Two resonances at $E_p = 1669$ and 1674 keV are observed in this region in the $(p\gamma)$ reaction. We measured the γ-decay spectra of both resonances and found that they have different natures: in the decay of the resonance at $E_p = 1669$ keV, the transition to the ground state (3/2⁻) is dominant, while in the decay of the resonance at $E_p = 1674$ keV the transition to the state at 1310 keV (7/2⁻) is the strongest. From the angular distributions of the direct transitions from the resonance at $E_p = 1674$ keV there follows uniquely the spin value 5/2 for this resonance. We assume that the resonance at $E_p = 1674$ keV carries the main part of the $T_>$ component of the $f_{5/2}$ analog.

The analog of the second excited state of ^{61}Ni (284 keV, 1/2⁻) must be situated in the region $E_p \approx 1.8$ MeV. Before our investigation, the excitation function had not been measured in this region, though measurements are known of the excitation function in the reaction ^{61}Ni(pp) with high proton resolution.[18] It was found[18] that at $E_p = 1856$ and 1875 keV there are excited two fine-structure components of the $p_{1/2}$ analog, these carrying the main strength of the $T_>$ state. A simplified state scheme of the parent nucleus ^{61}Ni, the analogs

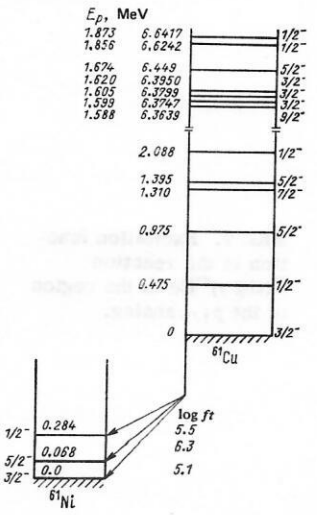

FIG. 5. Scheme of ^{61}Ni levels, their analogs in ^{61}Cu, and the low-lying states in ^{61}Cu.

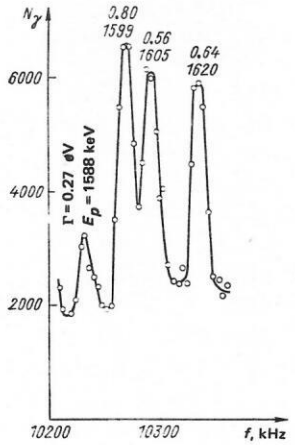

FIG. 6. Excitation function in the reaction $^{60}Ni(p\gamma)^{61}Cu$ in the region of the $p_{3/2}$ analog.

in ^{61}Cu, and the low-lying states of ^{61}Cu is shown in Fig. 5.

Excitation Functions and Gamma Decay Spectra of the Resonances. Isobar analog resonances were excited in the reaction $^{60}Ni(p\gamma)^{61}Cu$. We used a ^{60}Ni target (95% enrichment) of thickness 10 or 20 $\mu g/cm^2$. The excitation functions were measured only in the region of the analog resonances. In the region of the $p_{3/2}$ isobar analog resonance, the excitation function was measured in the range of proton energies (laboratory system) 1570–1640 keV; for the study of the $p_{1/2}$ analog, in the range E_p = 1830–1860 keV; and for the study of the $f_{5/2}$ analog, in the range 1650–1680 keV.

The excitation functions in the region of the $p_{3/2}$ and $p_{1/2}$ analogs are shown in Figs. 6 and 7. Note that near the two resonances at E_p = 1856 and 1873 keV observed in the (pp) reaction there is one further resonance at energy E_p = 1849 keV, which is not excited with appreciable cross section in proton elastic scattering. We measured the γ-decay spectra of the three resonances. The decay of the resonance at E_p = 1849 keV is characterized by a dominant transition to the ground state, in contrast to the decay of the other two resonances, for which the γ width of the transition to the ground state is only 10–20% of the total γ width. In view of these data, we conclude that the resonance at E_p = 1849 keV is not a fine-structure component of the $p_{1/2}$ analog.

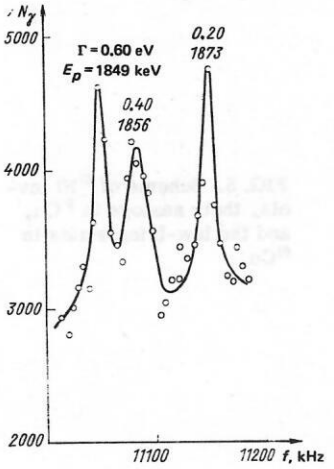

FIG. 7. Excitation function in the reaction $^{60}Ni(p\gamma)^{61}Cu$ in the region of the $p_{1/2}$ analog.

After the detection and identification of the isobar analog resonance, we measured its γ-decay spectra. Analysis of the γ spectra showed that up to 20 low-lying states of ^{61}Cu are populated by the decay of each resonance. The resonance decay schemes were constructed on the basis of the energy sums and differences with allowance for the intensities of the γ-transitions. The most reliable data correspond to the levels whose existence is known from various nuclear reactions.[28–30] The decay chain of a resonance is assumed to be established if we observe both the direct γ-transition from the resonance and also the transitions corresponding to de-excitation of the populated state. We constructed decay schemes of the $p_{3/2}$, $p_{1/2}$, and $f_{5/2}$ resonances and obtained data on the de-excitation scheme of the ^{61}Cu levels up to energies of order 3 MeV.[31]

Absolute Gamma Widths of the Resonances. The absolute values of the γ widths of the resonances were obtained by the thick-target method. We used a target of thickness 0.5 mg/cm^2, which corresponds to 45-keV energy loss for 1.6-MeV protons. The target enrichment was 95%. The yield of γ's was measured by means of a 100 × 100 mm NaI(Tl) crystal placed at a distance 70 mm from the target at an angle 90° to the proton beam. For the measurement of the excitation function, the detector recorded γ's with energy >3 MeV.

The excitation function is shown in Fig. 8. One can clearly identify three steps corresponding to resonance energies of the protons. For comparison, we show next to it the section of the excitation function measured by means of a target of thickness 1 keV.

To determine the absolute values of the decay probabilities of the resonances, we carried out an absolute calibration of the GeLi detector using an NaI(Tl) crystal whose absolute efficiency was known.

Using the NaI(Tl) detector at the resonance energy of the protons, we measured the region of the γ spectrum in which one could clearly identify the photopeak of the transition from the isobar analog resonance to the ^{61}Cu ground state (E_γ = 6.4 MeV).

Using the measured angular distributions (see below), we obtained the integrated intensity of the γ-transitions and determined the absolute yield of γ's corresponding to the transition from the isobar analog resonance to

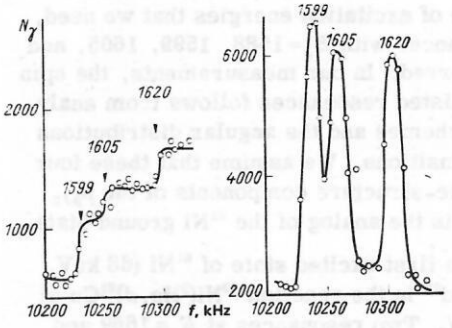

FIG. 8. Excitation function in the reaction $^{60}Ni(p\gamma)^{61}Cu$ measured with thick (on the left) and thin (on the right) targets.

the ^{61}Cu ground state. Simultaneously with the measurement of the γ spectra, we recorded the protons incident on the target, so that we could determine the number of emitted γ's of given energy per proton. The proton charge was measured by means of a calibrated integrator. Using the relation $\int \sigma dE = 2g\pi^2\lambda^2\Gamma_\gamma$ for $\Gamma_p \gg \Gamma_\gamma$, we determined the absolute values of the γ widths for transitions from the isobar analog resonance to the ground state.[21]

The total or partial γ widths for the other transitions from the isobar analog resonance can be obtained by using the relative intensities of the transitions determined in the measurements with the GeLi detector and thin target. Using the absolute calibration of the GeLi detector, we can determine the γ widths of the other resonances whose γ-decay was studied under the same conditions as the decay of the $p_{3/2}$ isobar analog resonance and for which the number of γ's of given energy per proton was measured.

The errors in the Γ_γ values are 20–30%. These are the rms errors taking into account the statistical spread and the errors in the determination of the detector efficiency, the intensity of the proton beam, and the solid angle. The main error is that in the determination of the solid angle subtended by the γ detector (12%).

Angular Distribution of the Gamma Rays. Measurements were made of the angular distributions of the γ's from the decay of the resonances with E_p = 1599, 1605, 1620, 1674, 1856, and 1873 keV be drawn about the spins of these resonances and the spins of some highly excited states of ^{61}Cu. The multipolarities were determined for many direct γ-transitions from each of the resonances to the ^{61}Cu levels.[23]

The γ's were recorded by a 40-cm^3 GeLi detector with energy resolution 7–8 keV for γ lines with energy 6.5 MeV. At given E_p, we measured the γ spectra at 90, 60, 30, 0° to the direction of the incident beam. For the measurement of the angular distributions of the gammas, we determined the intensity of the proton beam by the current integrator and we determined the integrated intensity of the gammas detected by the NaI(Tl) (100 × 100) crystal at 90° to the beam. This made it possible to normalize the intensity to both the number of protons passing through the target and to the number of γ's emitted from the target. The two normalizations gave results that agreed to within 0.5%, which indicates stable operation of the facility and reliability of the measurements.

The probability of emission of a γ ray in a nuclear reaction at angle θ to the direction of the incident particles is represented in the form of an expansion in Legendre polynomials:

$$W(\theta) = \sum_k a_k P_k(\cos\theta).$$

If a target with zero spin is used in the $(p\gamma)$ reaction and the excited state is an isolated resonance with definite spin value I^π, the coefficients a_k for direct γ emission depend only on the spins of the resonance and the final state and on the multipolarity admixture δ.

The angular distributions were evaluated as follows. The measured angular distributions, i.e., the counts at the corresponding peaks of the γ spectrum, normalized to the number of protons that passed through the target, were represented in the form of expansions in Legendre polynomials of degree not higher than four. The experimental values of the expansion coefficients a_2^{exp} and a_4^{exp} were found by the least-squares method. If the spins of the initial and final states are known, one can construct the dependence of a_k^{theor} on the multipolarity admixture and, from the curve $a_k^{theor}(\delta)$, determine the value of δ and its error. If the spin of the initial or the final state is unknown, one calculates the quantity

$$S(\delta) = \sum_{i=1}^{N} [Y_i(\theta_i) - W_i(\theta_i)]^2/\sigma_i^2,$$

where $Y_i(\theta_i)$ is the experimentally determined probability of γ emission at the angle θ_i, $W_i(\theta_i)$ is the theoretical value of this probability for a definite assumption about the unknown spin, and σ_i is the error of the measurements. The calculations were made under different assumptions about the value of the unknown spin and δ. The minimal value of S corresponds to the best choice of the values of the spin and δ. This value must satisfy the $\chi^2(N-P)$ distribution with $N-P$ degrees of freedom, where N is the number of independent measurements and P is the number of determined parameters. The reliability of the minimal S value can be determined by finding the probability for the occurrance of the S value for $N-P$ degrees of freedom from the $\chi^2(N-P)$ distribution. The error in δ can be determined by analyzing the behavior of $S(\delta)$ or from the dependence $a_k(\delta)$.

We studied the angular distribution of more than 60 γ lines corresponding to direct γ-transitions from the resonances to the low-lying ^{61}Cu states. In some cases, we obtained angular distributions for the photopeaks and the peaks of single and double emission of one γ-transition. As a rule, the corresponding coefficients a_k^{exp} agreed to within the errors.

In the cases when the analysis of the angular distributions of the γ's indicated that the resonance has spin 3/2, the results were re-evaluated in such a way as to describe the angular distribution by means of a single coefficient a_2 (for $J_{res} = 3/2$, $a_4 = 0$). The value of δ was determined from the value of this coefficient. For the decay of resonances with spin 3/2, two solutions, equally likely, are obtained for δ. Some measured angular distributions are shown in Figs. 9 and 10.

The spins of the resonances were determined from the angular distributions of the direct γ-transitions from the resonances to the low-lying states with energies 0.0 (3/2$^-$), 476 (1/2$^-$), 970 (5/2$^-$), 1395 (5/2$^-$), and 2089 keV (1/2$^-$). The spins of these states are well known. The angular distribution of one γ-transition does not, as a rule, uniquely determine the unknown spin of one of the states participating in the transition. However, in the case of γ-decay of resonances, several direct transitions from each resonance are observed. A combined analysis of the angular distributions of these transitions

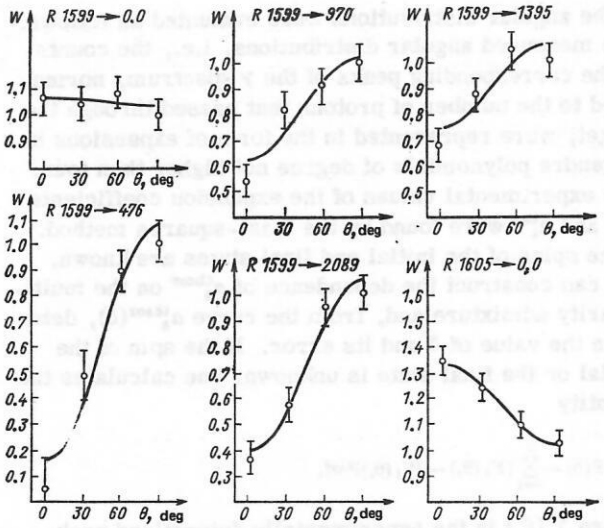

FIG. 9. Angular distributions of γ's resulting from the decay of resonances in ^{61}Cu.

can yield a unique determination of the spin of the resonance. Analysis of $S(J_i, \delta, J_k)$ shows that the angular distributions for the sequences $J_i \overset{\delta}{\to} 3/2$, $J_i \overset{\delta}{\to} 5/2$ give approximately the same χ^2_{min} for different J_i, i.e., they do not permit one to deduce the spin of the resonance. However, transitions to states with spin 1/2 ($J_i \overset{\delta}{\to} 1/2$) are very sensitive to the spin of the resonance. Figure 11 illustrates these properties. It can be seen from this figure that the spin of the resonance at $E_p = 1599$ keV is uniquely determined and equal to 3/2. Similarly, the spin values 3/2 are obtained for the resonances at $E_p = 1605$ and 1620 keV. The spin of the resonance at $E_p = 1674$ keV was found to be 5/2. This was deduced from an analysis of transitions to the 3/2 ground state and the 1310 keV (7/2) level. In the case of the resonances at $E_p = 1856$ and 1873 keV, the angular distributions were isotropic within the errors of the measurements. This agrees with a value 1/2 for the spins of these resonances, although other values of the spin can-

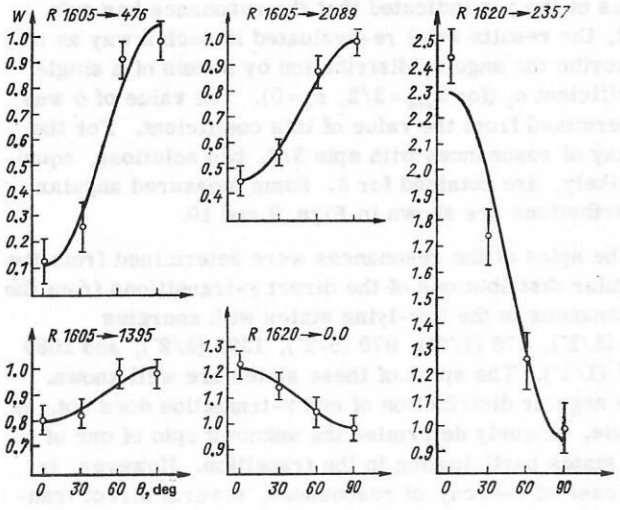

FIG. 10. Angular distributions of γ's resulting from the decay of resonances in ^{61}Cu.

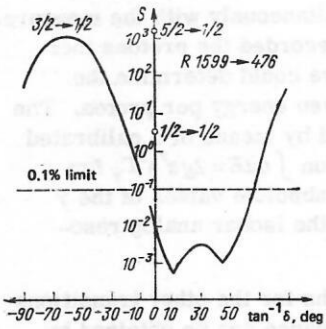

FIG. 11. The χ^2 analysis for the transition from the resonance at $E_p = 1599$ keV to the level with energy 476 keV.

not be eliminated on the basis of the measured angular distributions. The complete set of data on the γ-decay of the resonances, the data on the (pp) reaction,[18] and the angular distributions suggest 1/2 as the most probable spin of these resonances.

The spins of some ^{61}Cu excited states were established by analyzing the set of data on the reactions, the population and de-excitation of the states, and our measured angular distributions. The spins of the states at 2203 (5/2$^-$), 2357 (3/2$^-$), 2473 (3/2$^-$), 2584 (5/2$^-$), 2687 (3/2$^-$), and 2792 (5/2$^-$) are known from Ref. 29. Our data on the angular distributions of the direct transitions from the resonances to these states agree with the above spin values. The spins of the states 3002, 3022, 3062, and 3094 keV are in practice unknown. The measurements of the angular distributions enabled us to determine uniquely that the level at 3002 keV has spin 5/2. For the levels at 3022 and 3062 keV, the most probable spins are 1/2 and 3/2, respectively. The level at 3094 keV has spin 1/2 and 3/2.

The obtained values of the multipolarity admixtures make it possible to determine the partial γ widths separately for the $M1$ and $E2$ components. The partial widths determined in this manner and $B(M1)$ and $B(E2)$ are given in Table IV. Note that the $B(M1)$ values given in Table IV differ in the overwhelming majority of cases from the values obtained under the assumption of pure $M1$ transitions by 5–10%. The maximal difference, for three transitions, is 30%. As a rule, the values obtained for $B(E2)$ are 0.01–0.1 Weisskopf units.

Beta and Gamma Analog Transitions. As we have already said, there is a definite connection between the ft value for the β-transition and the $B(M1)$ value of the corresponding γ-transition from the analog. In the case of ^{61}Cu, the connection can be established for β-transitions from the ^{61}Cu ground state to some state in ^{61}Ni and for the γ-transition from the corresponding isobar analog resonance to the ^{61}Cu ground state.

In Table V we give the $B(M1, \sigma)$ values calculated from the known ft for the β-decay of ^{61}Cu and $B(M1)$ for the γ-decay of the isobar analog resonance. For the $p_{3/2}$ isobar analog resonance we give the sum over four fine-structure components. It can be seen that $B(M1)$ appreciably exceeds $B(M1, \sigma)$. According to the single-particle estimate, the enhancement for the $p_{3/2}$–$p_{3/2}$ gamma-transition may be by a factor 1.5 compared with the β-

TABLE IV. Partial widths for decay of analogs in ^{61}Cu.

$E_{res}-E_{lev}$, keV	J^{π}_{lev}	$\delta^2=\frac{E2}{M1}$	$\Gamma\cdot10^3$, eV	$\Gamma(E2)\cdot10^3$, eV	$\Gamma(M1)\cdot10^3$, eV	$B(E2)$, e^2fm^4	$B(M1)\cdot10^2$, μ_0^2
6375—0	3/2⁻	0.036	17.7	0.6±0.2	7±3	0.72	5.7
		256		17.6±3.0	$0.065^{+0.12}_{-0.05}$	20.7	0.02
6375—476	1/2⁻	0.053	8.3	$0.42^{+0.35}_{-0.15}$	7.9±2.0	0.72	3.3
		1600		8.3±2.0	0.0±0.1	14.4	0
6375—970	5/2⁻	0.029	6.4	0.2±0.2	6.2±1.4	0.5	3.4
		400		6.4±1.4	0.012±0.1	17.3	0.002
6375—1395	5/2⁻	0.014	12.9	0.18±0.16	12.7±2.7	0.75	8.9
		121		12.8±2.7	0.1±0.1	52	0.07
6375—2089	1/2⁻	0.0	4.6	0.0±0.1	4.6±1.0	0	5.1
		2.89		3.4±1.2	1.2±0.5	30	1.3
6375—2203	(5/2⁻)	0.09	5.1	0.01—0.42	4.7—5.1	0.01—4	5.5 ÷ 6.0
		9.61		$4.6^{+1.3}_{-2.0}$	$0.5^{+1.0}_{-0.5}$	46	0.56
6375—2473	3/2⁻	0.25	2.6	0.52±0.18	2.1±0.6	7.2	3.0
		25		2.5±0.7	$0.10^{+0.20}_{-0.05}$	35	0.15
6375—2584	5/2	0.01	3.9	0.04—0.5	$3.8^{+0.8}_{-1.3}$	0.6	6.2
		9.6		3.6±0.9	$0.4^{+0.1}_{-0.3}$	57	0.4
6375—2687	3/2⁻	0.09	2.7	0.22±0.16	2.4±0.8	4.0	4.2
		289		2.7±0.8	$0.0^{+0.05}_{-0.01}$	48	0
6375—2859	(1/2—5/2)⁻	0.0036	1.9	0.0±0.1	1.9±0.5	0	3.8
		4		1.5±0.5	0.38±0.25	35	0.75
6375—3022	(1/2—5/2)⁻	0.01	1.48	$0.015^{+0.040}_{-0.015}$	1.47+0.30	0.43	3.3
		9		1.34±0.40	$0.14^{+0.17}_{-0.05}$	39	0.3
6375—3062	(1/2—7/2)	0.029	1.48	$0.04^{+0.08}_{-0.04}$	1.44±0.4	1.3	3.4
		400		1,47±0.4	$0.01^{+0.06}_{-0.03}$	46	0.02
6375—3094	(1/2—5/2)⁻	0.022	2.5	0.06±0.02	2.4±0.5	1.8	5.9
		9		2.25±0.50	0.25±0.10	73	0.6
6380—0	3/2⁻	0.01	29	0.29±0.15	29±6	0.3	9.5
		49		28.5±6.0	0.6±0.3	33	0.2
6380—970	5/2⁻	0.00	28	0.00	2.8±0.6	0	1.5
		25		2.3±0.7	0.5±0.7	6.8	0.3
6380—1395	5/2⁻	0.00		0.00	10.0±2.2	0	7.0
		25	10.0	9.2±2.0	0.3±1.3	37	0.2—1
6380—2089	1/2	0.00		0.00	3.5±1	0	3.7
		4	3.5	$1.7^{+2.0}_{-0.5}$	$1.7^{+0.5}_{-2.0}$	15	1.9
6380—2473	3/2	0.04	2.0	$0.08^{+0.008}_{-0.06}$	1.9±0.5	1.0	2.8
		36		1.9±0.5	0.1±0.1	26	0.15
6380—2792	5/2	0.00	2.2	0.00	2.2±0.6	0	4.2
		25		2.0±0.9	$0.4^{+0.4}_{-0.9}$	43	0.8
6396—0	3/2	0.026	27	0.067±0.20	26±5	0.78	8.6
		100		27±5	0.26±0.50	30	0.1
6396—970	5/2	0.00	2.6	0.00	2.6±0.6	0	1.4
		16		2.4±0.8	$0.15^{+0.4}_{-0.1}$	6.4	0.08
6396—1395	5/2	0.00	9.2	0.00	9.2±1.8	0	6.4
		25		8.9±2.4	$0.3^{+0.8}_{-0.2}$	35	0.2
6396—2089	1/2	0.00	5.2	0.00	5.2±1.0	0	5.6
		2.25		$3.6^{+1.3}_{-1.7}$	$1.6^{+1.3}_{-0.9}$	30	1.7
6396—2357	3/2	0.026	1.47	0.47±0.04	1.43±0.35	0.42	1.9
		4		$1.2^{+0.4}_{-0.7}$	$0.3^{+0.5}_{-0.2}$	13.6	0.4
6396—2687	3/2	0.16	1.75	0.24±0.20	1.5±0.5	4.3	2.5
		81		$1.7^{+0.3}_{-1.0}$	0.05—0.75	30	1.1—1.3
6396—2859	(1/2—5/2)	0.025	4.7	0.10±0.06	4.6±0.9	2.3	9.0
		9		4.2±1.0	0.5±0.2	96	0.9
6449—0	3/2	0.00	0.56	0.00	0.56±0.12	0	0.17
		9		0.5±0.2	0.05±0.10	0.6	0.02
6449—970	5/2	0.096	10	$0.1^{+0.30}_{-0.06}$	$0.9^{+0.3}_{-0.5}$	0.23	0.5
		16		0.96±0.20	0.03±0.02	2.5	0.02
6449—1310	7/2	0.0025	4.9	$0.01^{+0.04}_{-0.01}$	4.9±1.0	0.04	3.0
		100		4.8±1.0	0.04±0.03	16.7	0.02
6449—1395	5/2	0.16	0.3	0.04±0.02	0.24±0.07	0.15	0.15
		49		0.29±0.06	0.00	1.1	0
6449—2203	(5/2)	0.04	4.5	0.17±0.15	4.3±0.9	1.5	4.8
		9		4.0±1.2	$0.4^{+0.5}_{-0.2}$	36	0.5
6449—2473	3/2	0.00	2.1	0.00	2.1±0.4	0	2.8
		9		1,9±0,6	$0.20^{+0.22}_{-0.07}$	23	0.28
6449—3002	(1/2—7/2)	0.01	1.4	0.014±0.008	1.4±0.4	0.4	2.9
6449—3062	(1/2—7/2)	0.0144	1.3	0.02±0.08	1.3±0.3	0.5	2.9

TABLE V. Beta and gamma analog transitions and analog–antianalog transitions in ^{61}Cu.

Analog	log ft	$B(M1,\sigma)$, μ_0^2	$B(M1)$, μ_0^2 analog-g.s.	$B(M1)$, μ_0^2 analog-$A\bar{A}$ (experiment)	$B(M1)$, μ_0^2 analog-$A\bar{A}$ (according to Eq. (52) of Ref. 4)
$p_{3/2}$	5.1	0.036	0.24	0.24	2.13
$f_{5/2}$	6.3	0.0015	0.0027	0.0047	0.014
$p_{1/2}$	5.5	0.028	0.024	0.057	0.094

transition. It is however known that the absolute value of the matrix element of the β-transition is approximately an order of magnitude less than the single-particle estimate. The hindrance is explained by the fact that there is a concentration of the strength of the β-transitions near the analog resonance. The hindrances for the β- and γ-transitions may be different.

From the relationship between the values of the reduced probabilities for the β- and γ-transitions ($p_{3/2}$ analog) a conclusion can be drawn about the influence of collective effects, i.e., mixing of the low-lying states with core polarization states.

For transitions from the $f_{5/2}$ and $p_{1/2}$ analogs, the $B(M1)$ and $B(M1,\sigma)$ values are approximately equal. This indicates that the l part makes a small contribution (in agreement with the single-particle estimates).

Analog–Antianalog Transitions. In ^{61}Cu, the antianalog states for the corresponding analogs may be identified as follows: the ground state ($3/2^-$) as the $p_{3/2}$ antianalog, the level at 476.4 ($1/2^-$) as the $p_{1/2}$ antianalog, and the level at 970 keV ($5/2^-$) as the $f_{5/2}$ antianalog. These states have large (greater than 0.6) spectroscopic factors in proton transfer reactions.

The experimental values of the probabilities of analog–antianalog transitions are given in Table V, in which we also give the values obtained without allowance for core polarization effects. It can be seen that the $p_{3/2}$ analog–antianalog transition is hindered by about a factor of ten. This hindrance is explained by the contribution of the core polarization states.

In nuclei of the *sd* shell, the intensity of the analog–antianalog transition corresponds to the single-particle estimate whereas in nuclei of the $f_{7/2}$ shell this transition is strongly hindered. In the decay of the $p_{3/2}$ isobar analog resonance in ^{61}Cu we encountered an intermediate case—hindrance by an order of magnitude.

The probabilities of $f_{5/2}$ and $p_{1/2}$ transitions agree with the single-particle estimates to within a factor 2.

The probabilities of analog– antianalog transitions of the type $p_{3/2}$, $p_{1/2}$, and $f_{5/2}$ in ^{61}Cu have not previously been calculated. We calculated these probabilities using the model described below. In Table VI, we give the energies, wave functions, and state population probabilities for the $p_{1/2}$ and $p_{3/2}$ analogs in ^{61}Cu. The calculations predict a slight hindrance of the $p_{3/2}$ analog–antianalog transition and a fairly appreciable hindrance of the $p_{1/2}$ analog–antianalog transition. For the $p_{3/2}$ transition, the predictions agree with the experiment. As regards the $p_{1/2}$ transitions, the experiment does not give such a strong hindrance. It should however be noted that the $p_{1/2}$ analog–antianalog transition is very weak. It is possible that the $T_<$ component of the analog makes an appreciable contribution to this transition.

For the decay of the $f_{5/2}$ analog, the results of the calculations are given in Table VII. The antianalog is also the lowest state. The calculation even predicts an enhancement of the analog–antianalog transition compared with the single-particle estimate. This effect is made possible by admixture of spin-flip states to the antianalog state. The experimental value is smaller than the one obtained by the single-particle estimate.

TABLE VI. Wave functions of ^{61}Cu states and transition probabilities for $p_{3/2}$ and $p_{1/2}$ analogs in ^{61}Cu.*

J^π	E_x, MeV	$p_{3/2}(f_{5/2}f_{5/2}^{-1})_{1^+}$	$p_{3/2}(p_{3/2}p_{3/2}^{-1})_{1^+}$	$p_{3/2}(p_{1/2}p_{3/2}^{-1})_{1^+}$	$p_{1/2}(f_{5/2}f_{5/2}^{-1})_{1^+}$	$p_{1/2}(p_{3/2}p_{3/2}^{-1})_{1^+}$	$p_{1/2}(p_{1/2}p_{3/2}^{-1})_{1^+}$	$p_{3/2}$ or $p_{1/2}$	$B(M1)$, μ_0^2 $p_{3/2}$	$B(M1)$, μ_0^2 $p_{1/2}$
$3/2^-$	−0.300	0.266	0.410	0.384	0.268	0.415	0.393	0.464	2.62	3.45
$1/2^-$	−0.467	0.356	0.548	0.376	0.176	0.267	0.254	0.515	1.49	0.55
$1/2^-$	−1.538	−0.199	−0.306	−0.277	0.378	0.574	0.563	−0.039	0.23	1.48
$3/2^-$	−1.586	−0.296	−0.453	−0.442	0.302	0.463	0.453	−0.036	1.06	1.84
$5/2^-$	−1.682	0.425	0.647	0.633	—	—	—	—	2.88	—
$1/2^-$	−3.580	−0.163	−0.280	0.873	0.017	0.026	0.160	−0.326	0.01	0.00
$3/2^-$	−3.694	0.009	0.036	−0.023	−0.345	−0.520	0.780	−0.015	0.00	0.004
$1/2^-$	−3.696	0.025	0.041	−0.090	−0.350	−0.531	0.765	−0.039	0.00	0.02
$3/2^-$	−3.819	−0.009	0.036	−0.025	0.837	−0.545	0.005	−0.006	0.00	0.81
$1/2^-$	−3.819	0.000	0.000	0.000	0.835	−0.550	0.000	0.000	0.00	0.41
$3/2^-$	−3.872	−0.334	−0.519	0.785	0.022	−0.029	0.041	−0.022	0.02	0.00
$5/2^-$	−3.874	−0.343	−0.532	0.774	—	—	—	—	0.03	—
$5/2^-$	−3.999	0.838	−0.546	−0.004	—	—	—	—	0.60	—
$3/2^-$	−3.999	0.840	−0.542	−0.003	0.019	−0.020	0.010	−0.001	0.40	0.00
$1/2^-$	−3.999	0.842	−0.539	−0.014	−0.001	−0.001	−0.001	0.003	0.19	0.00
$1/2^-$	−5.292	−0.312	−0.485	0.103	−0.079	−0.120	−0.094	0.792	0.10	0.00
$3/2^-$	−6.302	−0.158	−0.247	−0.201	−0.128	−0.212	−0.174	0.884	0.87	0.32

*$G_0=1$ MeV, $G_1=0.9$ MeV, $\Delta=1.0$ MeV, $\varepsilon_{ls}=0.2$ MeV. The energies are measured from the analog state.

TABLE VII. Wave functions of states and transition probabilities for the $f_{5/2}$ analog in ^{61}Cu.*

J^π	E_x, MeV	$f_{5/2}(f_{5/2}f_{5/2}^{-1})_{1^+}$	$f_{5/2}(p_{3/2}p_{3/2}^{-1})_{1^+}$	$f_{5/2}(p_{1/2}p_{3/2}^{-1})_{1^+}$	$f_{5/2}$	$B(M1)$, μ_0^2
5/2⁻	−1.292	0.405	0.622	0.596	0.308	1.86
3/2⁻	−1.681	0.426	0.649	0.631	—	1.29
7/2⁻	−1.681	0.426	0.649	0.631	—	2.56
7/2⁻	−3.875	−0.338	−0.533	0.776	—	0.03
5/2⁻	−3.875	−0.332	−0.522	0.786	−0.029	0.02
3/2⁻	−3.875	−0.338	−0.533	0.776	—	0.01
7/2⁻	−4.000	0.839	−0.543	−0.008	—	0.54
5/2⁻	−4.000	0.840	−0.543	−0.006	0.002	0.40
3/2⁻	−4.000	0.839	−0.543	−0.008	—	0.27
5/2⁻	−5.39	−0.143	−0.217	−0.169	0.951	0.10

*The conditions are the same as in Table VI.

This could indicate an overestimation of the admixture of spin-flip states in the antianalog state.

States of Core Polarization Type. The distributions of the quantities $B(M1)$ for transition from the analog to low-lying states are given in Figs. 12–14. The most striking feature revealed by the analysis of these distributions is the selective population of the states in ^{61}Cu, which arises because levels with large components of states of the core polarization type are involved in the γ-decay of the isobar analog resonance. A maximum in the strength function $B(M1)$ from the analogs shows up clearly for the decay of the $p_{1/2}$ analog. This was to be expected, since the probability of transition from the analog is distributed between transitions to the antianalog and core polarization states. For the $p_{1/2}$ analog, the transition to the antianalog has a low intensity, so that a manifestation of core polarization states is to be expected.

As can be seen from Table VI, at excitation energies 2.5–3 MeV there is a group of states with large components of the type $j_{n1}(j_p j_{n-1})_{1^+}$, $j_p = j_{n-1}$. The calculation was made for $\Delta = 1$ MeV. Making a small change of this parameter, one can achieve complete agreement between the average position of the core polarization states and the position of the maximum in the experimental distributions. The calculated $B(M1)$ distributions are given in Figs. 15 and 16. The complete sums of the quantities $B(M1)$ to core polarization states for the decay of the $p_{3/2}$, $p_{1/2}$, and $f_{5/2}$ analogs in ^{61}Cu are

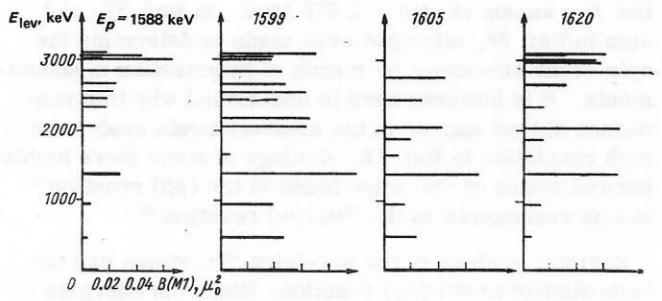

FIG. 12. Distribution of $B(M1)$ for transitions from the $p_{3/2}$ analog in ^{61}Cu (experiment).

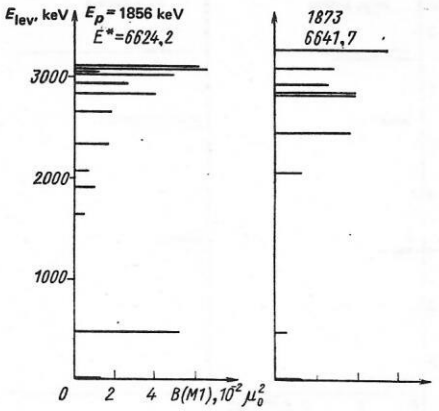

FIG. 13. Distribution of $B(M1)$ for transitions from the $p_{1/2}$ analog in ^{61}Cu (experiment).

equal to 1.3, 1.3, and $1.1\mu_0^2$, respectively, in accordance with the calculation. In the experimentally observed distributions, the $B(M1)$ sums are equal to 1.0, 0.5, and $0.1\mu_0^2$ for the same analogs.

Gamma-Decay of Fine-Structure Components of the Analogs. The $p_{3/2}$ and $p_{1/2}$ analog resonance in ^{61}Cu are split into several components. The distribution of the $T_>$ component of the analog, i.e., of the configuration of the actual analog state, over the $T_<$ states of the compound nucleus forms the fine structure of the analogs. The $p_{3/2}$ analog is distributed over four resonances. The strength of the $p_{1/2}$ analog ($T_>$ component) is mainly concentrated in two resonances. The wave functions of the analog resonances in the general case are a mixture of the $T_>$ and $T_<$ components. This circumstance is well known, but it is very difficult to obtain quantitative data on the relative contribution of each of the components to a given γ-transition. At the same time, it is clear that some transitions, especially the weakest, may be entirely determined by the $T_<$ component of the resonance and have no connection with the actual analog $T_>$ component at all.

At the present time, all theoretical predictions for the γ-decay of analogs ignore the possible manifestation of the $T_<$ component. In the experiments too, no attempts are made to separate the contributions of the $T_>$ and $T_<$ components. In the case of the $p_{3/2}$ analog in ^{61}Cu, we

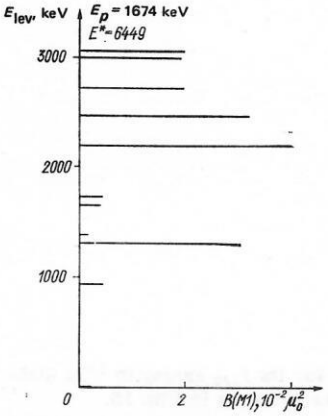

FIG. 14. Distribution of $B(M1)$ for transitions from the $f_{5/2}$ analog in ^{61}Cu (experiment).

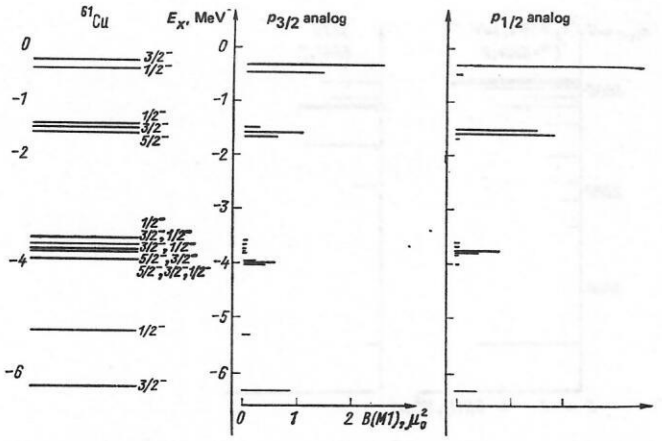

FIG. 15. Distribution of $B(M1)$ for $p_{3/2}$ and $p_{1/2}$ analogs in ^{61}Cu (calculation). The energies are measured from the position of the analog; $G_0 = 1.0$ MeV, $G_1 = 0.9$ MeV, $\Delta = 1.0$ MeV, $\varepsilon_{1s_{1/2}} = 0.2$ MeV.

made one of the first attempts at such estimates. In Ref. 33, we suggested that the correlation coefficient should be used to analyze the correlations between the partial γ widths for the decay of the analogs.

In the case of the decay of the $p_{3/2}$ analog in ^{61}Cu, it is natural to assume that the transition to the ground state is determined by the $T_>$ component. If the transitions to other states are also determined by this component, we should observe correlations between the partial γ widths. The results of the comparison show that correlations between the partial widths of the transitions to the ground state and to certain excited states are not observed. In contrast, we do observe correlations between the widths of the transitions to these states with one another and anticorrelations with the transition to the ground state.

The results can be explained as follows: The $T_<$ component of the resonance is not a complicated function of the compound nucleus but a relatively simple configuration which plays the role of a second (after the analog) doorway state.

One further feature of the decay of the fine-structure components of the analogs was manifested in our experiments. We found that the transition probabilities to the same state fluctuate rather strongly from resonance to

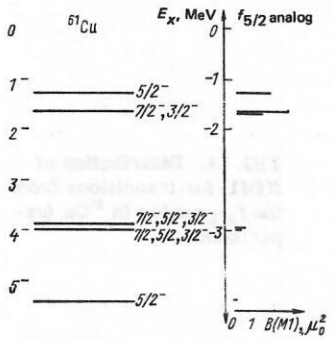

FIG. 16. Distribution of $B(M1)$ for the $f_{5/2}$ analog in ^{61}Cu (calculation). The conditions are the same as in Fig. 15.

resonance, though, as a rule, it is true that the same states are populated. Some ^{61}Cu states are not populated by the decay of any of the four resonances despite the absence of spin selection rules.

We mention one further circumstance which indicates a relatively simple structure of the nonanalog proton resonances. In the reaction, there is a fairly strong resonance at $E_p = 1849$ keV that is not observed in proton elastic scattering. The γ-decay of this resonance is distinguished by the dominant transition to the ground state.

4. GAMMA DECAY OF ANALOG RESONANCES IN ^{63}Cu

The energies, quantum numbers, and spectroscopic factors of the levels of the ^{63}Ni parent nucleus are well known. The levels of this nucleus have been frequently studied in neutron transfer reactions. The reaction ^{62}Ni$(dp)^{63}$Ni was investigated in Refs. 34–36. In contrast to ^{59}Ni and ^{61}Ni, the single-particle states are less clearly expressed in ^{63}Ni. For example, the strength of the $p_{1/2}$ state is distributed over many levels of the nucleus, two of them, with energy 0.0 and 1.003 MeV, having the largest spectroscopic factors, which are approximately equal. The $p_{3/2}$ and $f_{5/2}$ strengths are concentrated to a greater degree. The levels at 0.088 ($5/2^-$) and 0.155 MeV ($3/2^-$) carry the main strength of the $f_{5/2}$ and $p_{3/2}$ single-particle states. Despite the strong fragmentation of the single-particle strengths in ^{63}Ni, we shall still say that the ground state, the first excited state, and the second excited state are $p_{1/2}$, $f_{5/2}$, and $p_{3/2}$ states. In ^{63}Ni, the single-particle $g_{9/2}$ state is at 1.29 MeV.

The analog of the ground state of ^{63}Ni ($1/2^-$) was identified in Ref. 18, in which the excitation function in elastic scattering of protons on ^{62}Ni was investigated. At $E_p = 2481$ keV, there is observed a strong $1/2^-$ resonance ($\Gamma_p = 180$ eV), carrying the main strength of the $T_>$ component of the $p_{1/2}$ analog. The same investigation identified the analog of the second excited state of ^{63}Ni ($3/2^-$) with energy 0.155 MeV. This analog, which is fragmented over several components, is observed at $E_p \approx 2660$ keV. The main strength is concentrated in two resonances with $J^\pi = 3/2^-$ at $E_p = 2658$ and 2659 keV. The analog of the first excited state of ^{63}Ni (88 keV, $5/2^-$) is not observed in the proton elastic scattering reaction, this apparently being due to the large centrifugal barrier for $l_p = 3$. In Ref. 37, it is asserted that the $f_{5/2}$ analog is at $E_p = 2.576$ MeV. In Ref. 37, and also in Ref. 38, attempts were made to determine the spin of the resonance by means of polarization measurements. It is however hard to understand why this resonance did not appear in the measurements made with high resolution in Ref. 18. Analogs of some more highly excited states of ^{63}Ni were found in the (pp) reaction[18] and as resonances in the ^{62}Ni(pn) reaction.[39]

Earlier, analogs of the low-lying ^{63}Ni states had not been studied in the $(p\gamma)$ reaction. Since the energies of the $p_{1/2}$ and $p_{3/2}$ analogs were established with an error of 2–3 keV in the proton elastic scattering reaction, it

was not difficult to identify them in the $(p\gamma)$ reaction. Harder was the search for the $f_{5/2}$ analog, whose position was not established in the (pp) reaction. However, it could be detected in the $(p\gamma)$ reaction. The approximate position of the $f_{5/2}$ analog can be estimated if the position of the analog of the ^{63}Ni ground state is known. However, the uncertainty of this estimate is 30–40 keV (it is associated with the uncertainty in ΔE_c, which is the difference of the Coulomb energies).

Our measurement of the excitation function in the corresponding energy region revealed three strong resonances at E_p = 2546, 2556, and 2568 keV.[40-42] The nature of their γ-decay indicates that the resonances at E_p = 2546 and 2556 keV are components of the split $f_{5/2}$ analog. The γ-decay of these resonances is characterized by intense population of states with spins 3/2, 5/2, and 7/2, whereas the γ-decay of the resonance at E_p = 2586 keV is characterized by strong transitions to levels with spins 1/2. The spin value 5/2 for the resonance at E_p = 2556 keV follows unambiguously from the angular distributions of the direct γ-transitions from the resonance to the ^{63}Cu levels and the γ de-excitation of this resonance.

There have been recent studies of the $p_{1/2}$ and $p_{3/2}$ analogs in the $(p\gamma)$ reaction.[43,44]

The scheme of the ^{63}Ni levels, their analogs in ^{63}Cu, and the low-lying levels of ^{63}Cu are shown in Fig. 17.

Excitation Functions and Gamma-Decay Spectra of Analogs. The excitation functions in the reaction ^{62}Ni$(p\gamma)$ were studied under the same conditions as in the reactions ^{58}Ni$(p\gamma)$ and ^{60}Ni$(p\gamma)$. The γ's were detected by a 100 × 100 mm NaI(Tl) crystal. A ^{62}Ni target of thickness 10 μg/cm^2 was used for the measurements. Since the form of the excitation function in the region of proton energies of interest to us was not known, we made series of measurements with different discrimination thresholds for the energies of the γ's detected by the NaI(Tl) crystal. Some excitation functions were measured for a definite interval of γ energies selected by means of an analyzer. The excitation functions were measured in the interval E_p = 2440–2680 keV. In this range of proton energies, there are $p_{1/2}$, $f_{5/2}$, and $p_{3/2}$ analog resonances. Figure 18 shows a section of

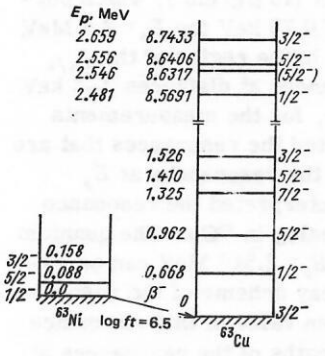

FIG. 17. Scheme of ^{63}Ni levels, the analogs in ^{63}Cu, and the low-lying states of ^{63}Cu.

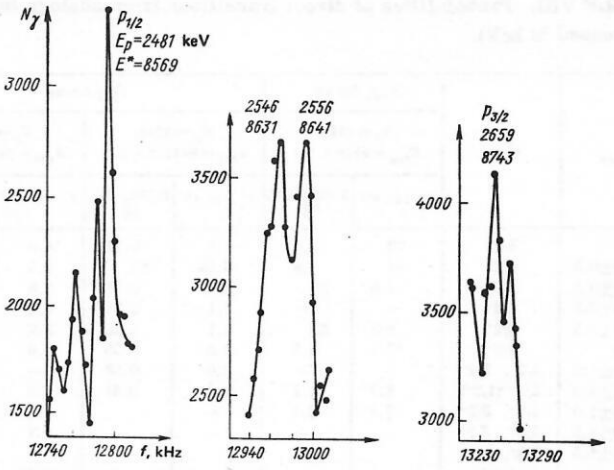

FIG. 18. Excitation function in the reaction ^{62}Ni$(p\gamma)^{63}$Cu in the neighborhood of analog resonances.

the excitation function in the neighborhood of the $p_{1/2}$ analog (E_p = 2460–2490 keV). At E_p = 2481 keV, a peak corresponding to the $p_{1/2}$ analog can be seen. In the same manner, we identified the $p_{3/2}$ analog at excitation energy E_p = 2659 keV. As we have already noted, the $f_{5/2}$ analog was identified at energies E_p = 2546 and 2556 keV. In the neighborhood of the $p_{1/2}$ analog, several resonances with energies E_p = 2455, 2469, 2476, 2492, and 2516 keV were also observed. The first four of these resonances were observed in proton elastic scattering,[18] in which they were ascribed the quantum numbers $1/2^+$. The resonance at E_p = 2516 keV and also some other resonances in the investigated range of proton energies were not observed in elastic scattering, although they were fairly strong in the $(p\gamma)$ reaction.

The γ-decay spectra of the resonances were measured for three analogs with E_p = 2481 ($p_{1/2}$), 2546 and 2556 ($f_{5/2}$), and 2659 keV ($p_{3/2}$) for a series of resonances around the $p_{1/2}$ analog (E_p = 2455, 2469, 2476, 2492, and 2516 keV), and also near the $f_{5/2}$ analog (E_p = 2586 keV). The γ spectra were measured with 40-cm^3 GeLi detectors of resolution 10–12 keV for 8.5-MeV gammas.

In the spectrum of each resonance, we observed more than 100 lines, including both direct γ-transitions from the resonances as well as γ's belonging to de-excitation of low-lying states. The decay of the analogs and other resonances that we studied resulted in the population of about 40 levels in ^{63}Cu with energies up to 4 MeV. For each resonance, a decay scheme, balanced with respect to the energies and intensities, was constructed. In constructing the decay schemes, we used the energies of the low-lying ^{63}Cu states known[45] from the decay of ^{63}Zn, and levels with higher excitation energies known from the proton inelastic scattering reaction on ^{63}Cu.[46,47] In Table VIII, we give data on direct population of the ^{63}Cu levels from analog resonances. In the first column, we give the energies obtained from our measurements together with the rms error. The greater part of the low-lying states up to 3100 keV was observed in the β-decay of ^{63}Zn. Exceptions are the states with energies 2405, 2678, 2831, 2956, and 2978 keV. These

TABLE VIII. Probabilities of direct transitions from analogs in ^{63}Cu (the energy is expressed in keV).

E_{lev}	J^{π}_{lev}	$p_{1/2}$ Analog		$f_{5/2}$ Analog				$p_{3/2}$ Analog	
		$E_p = 2481$, $E_{res} = 8569 \pm 1.5$		$E_p = 2546$, $E_{res} = 8631.7 \pm 2.0$		$E_p = 2556$, $E_{res} = 8640.6 \pm 2.0$		$E_p = 2659$, $6E_{res} = 8743.3 \pm 1.5$	
		$\Gamma_\gamma \cdot 10^3$, eV	$B\,(M1) \cdot 10^3$, μ_0^2	$\Gamma_\gamma \cdot 10^3$, eV	$B\,(M1) \cdot 10^3$, μ_0^2	$\Gamma_\gamma \cdot 10^3$, eV	$B\,(M1) \cdot 10^3$, μ_0^2	$\Gamma_\gamma \cdot 10^3$, eV	$B\,(M1) \cdot 10^3$, μ_0^2
0	3/2⁻	22	3.0	1.8	0.24	4.6	0.61	6.0	0.77
668.3±0.5	1/2⁻	11	1.9	0.25	*E2*	1.0	*E2*	5.0	0.82
961.6±0.5	5/2⁻	2.6	*E2*	2.0	0.38	2.8	0.56	7.9	1.45
1325.6±0.5	7/2⁻	—	—	1.1	0.24	1.4	0.31	1.1	*E2*
1410.4±0.5	5/2⁻	5.5	*E2*	1.1	0.25	2.9	0.66	4.6	1.0
1546.5	3/2⁻	17	4.3	2.3	0.55	2.6	0.63	1.8	0.41
1860.0±1.0	5/2⁻, 7/2⁻	—	—	1.0	0.28	—	—	—	—
2012.2±1.0	3/2⁻ (1/2⁻)	3.7	1.1	1.4	0.41	0.8	0.24	1.6	0.45
2060.0±1.0	1/2⁻, 3/2⁻	7.7	2.4	—	—	1.1	*E2*	0.8	0.23
2080.0±1.5	5/2⁻, 3/2⁻	—	—	—	—	1.1	0.33	1.3	0 38
2333.6±1.5	3/2⁻, 5/2⁻, 1/2⁻	—	—	—	—	0.87	0.30	1.6	0.52
2405 ±3	—	1.9	0.69	—	—	—	—	—	—
2497.3±1.5	3/2⁻	10	3.9	—	—	1.5	0.56	0.4	0.13
2533.7±2.0	5/2⁻, 3/2⁻	0.7	0.27	—	—	2.2	0.83	0.9	0.32
2677.9±1.8	—	9.9	4.2	—	—	0.8	0.32	1.7	0.66
2697±2	1/2⁻, 3/2⁻, 5/2⁻	5.1	2.2	—	—	—	—	—	—
2778±2	3/2⁻, 5/2⁻, 1/2⁻	—	—	—	—	1.2	0.51	—	—
2831±2	—	—	—	1.0	0.39	—	—	—	—
2860±2	1/2⁻, 3/2⁻, 5/2±	—	—	—	—	—	—	2.4	1.0
2886±2	1/2⁻, 3/2±, 5/2⁻	3.3	1.6	—	—	0.7	0.32	0.8	0.30
2956±3	—	3.3	1.6	—	—	—	—	1.1	0.49
2978.6±1.6	—	2.6	1.3	—	—	—	—	0.9	0.40
3042±3	1/2±, 3/2±, 5/2±	3.5	1.8	—	—	1.6	0.78	0.4	0.43
3100±3	1/2±, 3/2±, 5/2±	4.4	2.3	—	—	0.9	0.46	—	—
3127±3	—	—	—	—	—	0.9	0.46	—	—
3224±3	—	4.8	2.7	—	—	0.9	0.49	1.6	0.82
3264±3	—	1.6	0.90	—	—	1.3	0.72	—	—
3292±4	—	5.7	3.0	—	—	1.1	0.62	2.4	1.3
3309±4	—	7.5	4.5	0.7	0.40	2.5	1.42	3.8	2.0
3406±3	—	3.5	2.2	—	—	—	—	—	—
3429±2	—	4.8	3.0	—	—	—	—	—	—
3461±4	—	3.7	2.4	—	—	—	—	4.2	2.4
3476±4	—	—	—	—	—	—	—	1.8	1.1
3535±3	—	—	—	—	—	—	—	1.6	0.78
3657±4	—	4.4	3.2	—	—	—	—	—	—
3774±4	—	2.6	2.0	—	—	—	—	—	—
3902±3	—	—	—	—	—	—	—	2.0	1.5
3960±3	—	—	—	—	—	—	—	1.8	1.4
4058±5	—	—	—	—	—	—	—	2.2	1.8
4119±5	—	—	—	—	—	—	—	4.6	4.0

Note. The values of the resonance strengths $(2J+1)\Gamma_p\Gamma_{\gamma 0}/\Gamma$ are determined with an error 20% for an angle 90° between the directions of the γ ray and the incident beam. The Γ_γ are given without allowance for the angular distribution.

levels and the levels with energies >3000 keV were observed in proton inelastic scattering. The level at 3264 keV is introduced for the first time.

The values of the quantum numbers in the second column of Table VIII are taken from Ref. 45. For the remaining levels, the J^π values are unknown. In the construction of the decay schemes, we traced the γ de-excitation of the low-lying states.

Absolute Values of the Partial Gamma Widths. The absolute values of the partial γ widths in ^{63}Cu were measured by the thick-target method. In the reaction ^{62}Ni$(p\gamma)^{63}$Cu, analog resonances are situated in the region of excitation energies of the compound nucleus around 8.5 MeV. In this region, the level density is greater than in the case of ^{61}Cu. In the excitation function obtained with a thin target (10 μg/cm^2), which corresponds to an energy loss of 0.75 keV for E_p = 2.5 MeV, resonance peaks are situated in the region of the $p_{1/2}$ and $p_{3/2}$ isobar analog resonances at distances 2–3 keV from one another. Therefore, for the measurements with the thick target we selected the resonances that are fairly well isolated, namely, the resonances at E_p = 2.556 and 2.516 MeV. We interpreted the resonance at E_p = 2.556 MeV as a $f_{5/2}$ analog in ^{63}Cu. The quantum numbers of the resonance at E_p = 2.516 MeV can be established by analyzing the decay scheme of the resonance. The most probable spin value of this resonance is 3/2. Determining the strengths of the resonances at 2.516 and 2.556 MeV in the direct manner, we can obtain the strengths of the other resonances.

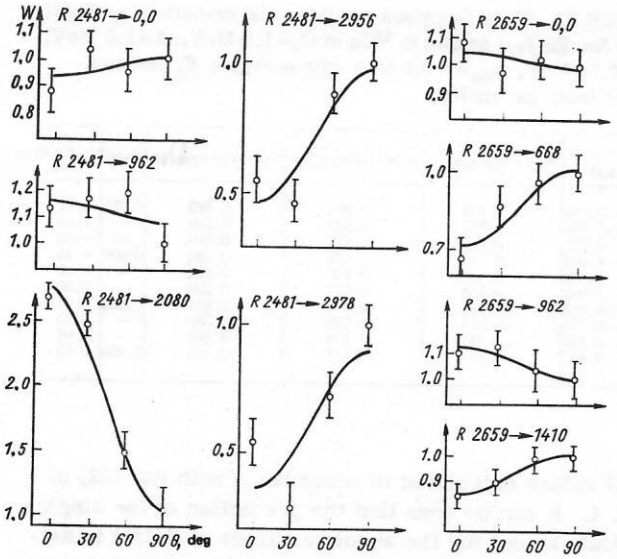

FIG. 19. Angular distributions of some γ-transitions from analogs in ^{63}Cu.

Angular Distribution of the Gammas. We measured the angular distributions of direct γ-transitions from the analogs in ^{63}Cu to low-lying states for the resonances at E_p = 2481, 2566, and 2569 keV.[48] The main task in measuring the angular distributions is to determine the spins of the resonances manifested in the $(p\gamma)$ reaction. The quantum numbers of the resonances at E_p = 2481 and 2659 keV were determined from proton elastic scattering. However, some indirect data suggest that the resonance revealed in the $(p\gamma)$ reaction at E_p = 2481 keV is an unresolved doublet of two states with spins 1/2 and 3/2 or 5/2. The angular distributions confirmed such an assumption. In the case of the resonance at E_p = 2659 keV, the angular distributions gave a unique determination 3/2 of its spin, confirming the elastic scattering data. For the resonance at E_p = 2556 keV, we obtained the unambiguous spin 5/2. For γ-transitions from the resonances at E_p = 2556 and 2649 keV, we determined the multipolarity admixtures δ.

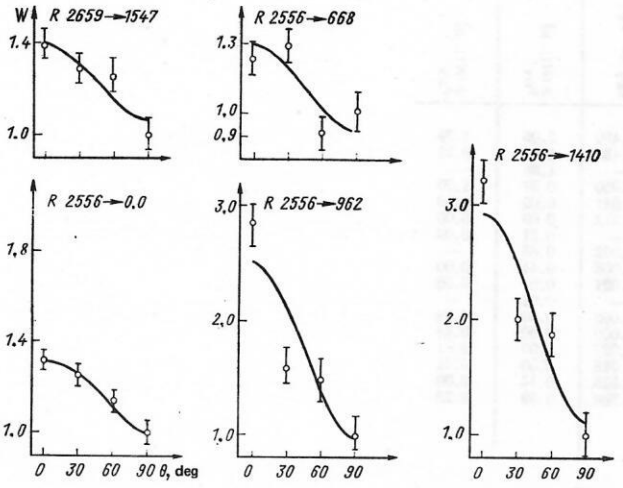

FIG. 20. Angular distributions of γ-transitions from analogs in ^{63}Cu.

The angular distributions were measured under the same conditions as in the case of ^{61}Cu for angles 0, 30, 60, and 90° to the direction of the proton beam.

For the decay of the analogs in ^{63}Cu, we studied the angular distributions of more than 50 γ-ray lines in the decay spectra of the resonances. The angular distributions of some transitions are shown in Figs. 19 and 20 as an illustration.

The angular distributions of direct γ-transitions from the resonance at E_p = 2481 keV (1/2⁻) should be isotropic. In fact, for the majority of transitions we obtained a_2 values that agree with the value a_2 = 0 within the errors. However, transitions to some levels are strongly asymmetric. This large asymmetry cannot be explained by any experimental errors. It is natural to assume that the resonance at E_p = 2481 keV observed in the $(p\gamma)$ reaction is complex and consists of a doublet of states. One of them, with spin 1/2⁻, appears with considerable strength in the proton elastic scattering reaction; the other, with spin 3/2 or 5/2, is excited together with the first state in the $(p\gamma)$ reaction.

The angular distributions of the direct γ-transitions from the resonance at E_p = 2659 keV give a definite spin value of this resonance equal to 3/2. This follows from the analysis of the angular distribution of the transition from the resonance to the level at 668 keV (1/2⁻) (Fig. 21).

The spin of the resonance at E_p = 2556 keV can also be unambiguously determined from the angular distributions of transitions to different levels.

We also measured the angular distributions of the γ transitions in the decay of some resonances near the $p_{1/2}$ analog.[49] We studied the resonances at the proton energies E_p = 2455, 2469, 2476, 2492, and 2516 keV. The first four resonances in the proton elastic scattering reaction were ascribed the quantum numbers 1/2⁺. However, analysis of the γ de-excitation of the resonances suggests that their spin values are restricted to 3/2 and 5/2.

The data on the angular distributions indicate a strong asymmetry for some γ-transitions from these resonances. This rules out the spin value 1/2 for the resonances E_p = 2455, 2469, 2476, 2492, and 2516 keV. Taken together, the data on the de-excitation and the angular distributions indicate that in the reactions (pp) and $(p\gamma)$ we have excitation of different resonances that have the same energy to within the errors.

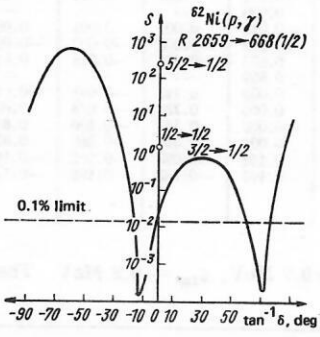

FIG. 21. The χ^2 analysis for the transition from the resonance at E_p = 2659 keV to the level with energy 668 keV in ^{63}Cu.

TABLE IX. Analog–antianalog transitions in ^{63}Cu.

Analog	$B(M1)$, μ_0^2	
	Experiment	Calculation in accordance with Eq. (52) of Ref 4
$p_{1/2}$	0.019	0.077
$f_{5/2}$	0.0185	0.011
$p_{3/1}$	0.0077	1.70

Beta and Gamma Analog Transitions. The nucleus ^{63}Ni ($1/2^-$) decays to the ground state of ^{63}Cu ($3/2^-$). The value of log ft for this transition is 6.5. The analog for it is the γ-transition from the $p_{1/2}$ analog to the ^{63}Cu ground state. The value of $B(M1, \delta)$ calculated from the ft value is $0.001\,\mu_0^2$. The experimental value of $B(M1)$ for the transition from the resonance at E_p = 2481 keV to the ^{63}Cu ground state is $0.03\,\mu_0^2$. The value of the ratio $B(M1)/B(M1, \delta)$ is 30.

The systematics of the ratios $B(M1)/BM1, \delta)$ given in Ref. 4 shows that as a rule this ratio is greater than 1; in the majority of cases, it is between 1 and 5. The value of the ratio $B(M1)/B(M1, \delta)$ for ^{63}Cu is the largest. From this, one could conclude that the l part makes an appreciable contribution in this transition. However, it must be borne in mind that the angular distributions of the γ-transitions from this resonance indicate that the resonance has a complicated nature. It would seem that this explains the anomalously large value of $B(M1)/B(M1, \delta)$.

Analog-Antianalog Transitions. In the ^{63}Cu nucleus, the antianalogs for the $p_{1/2}$, $f_{5/2}$, and $p_{3/2}$ analogs can be taken to be the levels at 668 ($1/2^-$, S = 0.71), 962 ($5/2^-$, S = 0.29), and 1410 keV ($5/2^-$, S = 0.34), and the ground state ($3/2^-$, S = 0.78). The experimental values of the analog–antianalog transition probabilities in ^{63}Cu are given in Table IX, in which we also give the theoretical values calculated in accordance with Eq. (52) of Ref. 4. It can be seen that the prediction of the single-particle model for the absolute values of $B(M1)$ is satisfied in order of magnitude in the case of the transitions $p_{1/2} \to p_{1/2}$ and $f_{5/2} \to f_{5/2}$. For the $p_{3/2}$ analog, the analog–antianalog transition is observed to be hindered by more than two orders of magnitude.

TABLE XI. Wave functions of states and transition probabilities for the $f_{5/2}$ analog in ^{63}Cu at G_0=1.0 MeV, Δ=1.0 MeV, G_1=0.70 MeV, ϵ_{lsp}=−0.2 MeV (the energies E_x are measured from the analog).

J^π	E_x, MeV	$f_{5/2}(f_{5/2}f_{5/2}^{-1})_{1+}$	$f_{5/2}(p_{3/2}p_{3/2}^{-1})_{1+}$	$f_{5/2}(p_{1/2}p_{3/2}^{-1})_{1+}$	$f_{5/2}$	$B(M1)$ μ_0^2
5/2−	−3.665	0.555	0.604	0.493	0.292	1.21
7/2−	−3.976	0.582	0.633	0.510	—	1.65
3/2−	−3.976	0.582	0.633	0.510	—	0.83
5/2−	−6.001	0.736	−0.677	0.000	0.000	0.44
7/2−	−6.001	0.736	−0.677	0.000	—	0.59
3/2−	−6.001	0.736	−0.677	0.000	—	0.30
5/2−	−6.142	−0.354	−0.385	0.851	0.033	0.01
7/2−	−6.144	−0.345	−0.376	0.860	—	0.01
3/2−	−6.144	−0.345	−0.376	0.860	—	0.01
5/2−	−7.313	−0.157	−0.171	−0.180	0.956	0.05

In a model with residual interaction (see below) one can qualitatively explain the hindrance of both the $p_{1/2}$ and the $p_{3/2}$ analog-antianalog transitions. In Table X we give the energies, wave functions, and state population probabilities for decay of the $p_{1/2}$ and $p_{3/2}$ analogs in ^{63}Cu. The analog-antianalog transition of type $p_{3/2}$ is hindered but the hindrance is much less than the value observed experimentally. The analog–antianalog transition of type $p_{1/2}$ is hindered more strongly than is observed experimentally.

For the $f_{5/2}$ analog, data are given in Table XI. In the case of the $f_{5/2}$ analog–antianalog transition, the experimental value is larger than the single-particle value. The value calculated in the model with residual interaction is also larger than the single-particle unperturbed quantity.

TABLE X. Wave functions of states and transition probabilities for $p_{1/2}$ and $p_{3/2}$ analogs in ^{63}Cu.*

J^π	E_x, MeV	$p_{3/2}(f_{5/2}f_{5/2}^{-1})_{1+}$	$p_{3/2}(p_{3/2}p_{3/2}^{-1})_{1+}$	$p_{3/2}(p_{1/2}p_{3/2}^{-1})_{1+}$	$p_{1/2}(f_{5/2}f_{5/2}^{-1})_{1+}$	$p_{1/2}(p_{3/2}p_{3/2}^{-1})_{1+}$	$p_{1/2}(p_{1/2}p_{3/2}^{-1})_{1+}$	$p_{3/2}$ or $p_{1/2}$	$B(M1)$, μ_0^2 $p_{3/2}$	$B(M1)$, μ_0^2 $p_{1/2}$
3/2−	−2.978	0.414	0.451	0.377	0.297	0.328	0.275	0.460	2.05	1.79
1/2−	−3.023	0.504	0.548	0.350	0.167	0.181	0.152	0.489	1.04	0.21
5/2−	−3.981	0.582	0.632	0.512	—	—	—	—	1.86	—
3/2−	−4.110	−0.353	−0.384	−0.310	0.461	0.501	0.408	0.050	0.37	1.70
1/2−	−4.167	−0.203	−0.220	−0.191	0.544	0.589	0.479	0.041	0.00	1.10
1/2−	−5.993	−0.179	−0.231	0.911	0.061	0.066	0.054	−0.272	0.00	0.00
5/2−	−5.996	0.736	−0.677	0.000	—	—	—	—	0.21	0.00
3/2−	−5.996	0.744	−0.668	−0.018	0.001	0.001	0.000	−0.002	0.66	—
1/2−	−5.996	0.740	−0.672	−0.022	−0.002	−0.002	−0.001	0.008	0.44	0.00
3/2−	−6.142	−0.389	−0.402	0.850	−0.016	−0.019	0.012	0.021	0.01	0.00
5/2−	−6.143	−0.347	−0.377	0.859	—	—	—	—	0.01	—
3/2−	−6.211	0.003	0.004	0.003	0.745	−0.667	−0.013	−0.008	0.00	0.89
1/2−	−6.211	0.000	0.000	0.000	0.735	−0.678	0.000	0.000	0.00	0.44
3/2−	−6.357	−0.002	−0.002	−0.030	−0.343	−0.400	0.849	0.027	0.00	0.01
1/2−	−6.358	−0.011	−0.011	0.001	−0.351	−0.380	0.856	0.018	0.00	0.01
1/2−	−7.354	−0.358	−0.382	0.102	−0.098	−0.106	−0.114	0.828	0.14	0.00
3/2−	−8.093	−0.185	−0.204	−0.197	−0.162	−0.192	−0.192	0.886	0.69	0.23

*G_0=1.0 MeV, Δ=1.0 MeV, G_1=0.7 MeV, ε_{lsp}=−0.2 MeV. The energies E_x are measured from the analog.

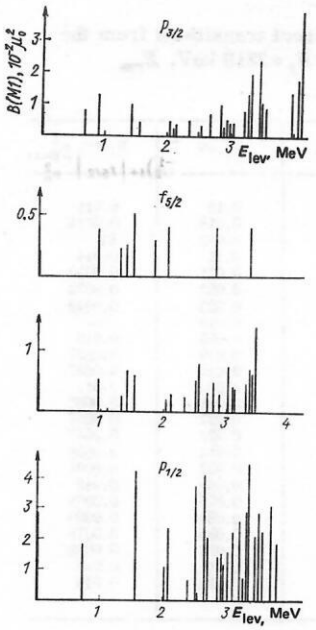

FIG. 22. Strength functions for $M1$ transitions from the $p_{3/2}$, $f_{5/2}$, and $p_{1/2}$ analogs in ^{63}Cu (experiment).

States of Core Polarization Type. The strength functions for the decay of the $p_{3/2}$, $f_{5/2}$, and $p_{1/2}$ analogs in ^{63}Cu are given in Fig. 22. It must however be recalled that in the case of the $p_{1/2}$ analog the resonance at $E_p = 2481$ keV is complex. From the experimental point of view, the decay of the resonance at $E_p = 2481$ keV is not the pure decay of a $p_{1/2}$ analog. A maximum in the distribution of the transition probabilities is observed for the $p_{3/2}$ analog and, less clearly, for the $f_{5/2}$ and $p_{1/2}$ analogs. The maximum is observed for transitions to levels with excitation energies 3.5 MeV. The excitation energies of the analogs are equal to 8.6 MeV. The calculated distributions of the $B(M1)$ values for transitions from the analogs are given in Figs. 23 and 24 ($\Delta = 1.0$ MeV). For $\Delta = 2.0$ MeV, the excitation energy of the core polarization state is equal to the energy of the maximum in the experimental distributions. The sum of the $B(M1)$ values from the $p_{3/2}$, $f_{5/2}$, and $p_{1/2}$ analogs to all core polarization states was found to be approximately the same for all analogs and equal to $1.3\,\mu_0^2$. The corresponding experimental values are 0.3, 0.3, and $0.1\,\mu_0^2$. The last value is the total $B(M1)$ sum observed for decay of the $f_{5/2}$ analog.

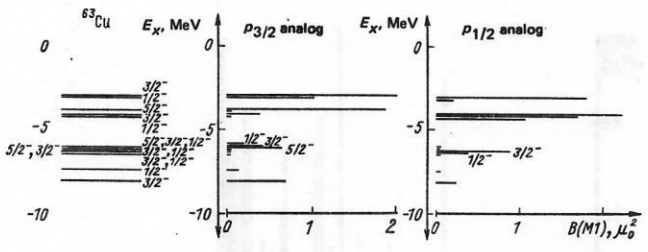

FIG. 23. Strength functions of $M1$ transitions from $p_{3/2}$ and $p_{1/2}$ analogs in ^{63}Cu (calculation). The energies are measured from the position of the analog; $G_0 = 1.0$ MeV, $G_1 = 0.7$ MeV, $\Delta = 1.0$ MeV, $\varepsilon_{lsp} = -0.2$ MeV.

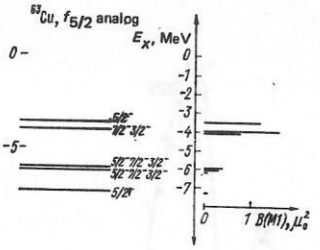

FIG. 24. Strength function of $M1$ transitions from the $f_{5/2}$ analog in ^{63}Cu (calculation). The conditions are the same as in Fig. 23.

5. GAMMA DECAY OF ANALOG RESONANCES IN ^{65}Cu

The ^{65}Ni parent level whose analog we studied is a level with energy 0.064 MeV, which carries the main single-particle $p_{1/2}$ strength: $(2J+1)S(dp) = 1.23$ (Ref. 35).

Analog states in ^{65}Cu have been studied on a number of occasions. In Refs. 39 and 50, analogs of the ^{65}Ni levels were studied in the reaction ^{64}Ni$(pn)^{64}$Cu, and $f_{5/2}$, $p_{1/2}$, $p_{3/2}$, and $d_{5/2}$ analogs corresponding to the ground state of ^{65}Ni and states with energies 0.064, 0.692, and 1.92 MeV, respectively, were found.

In Ref. 51, the (pp) and (pp') reactions on ^{64}Ni were investigated. Analogs of the $p_{1/2}$, $p_{3/2}$, and $d_{5/2}$ levels were identified. In Ref. 18, proton elastic scattering on ^{64}Ni was investigated for E_p in the range from 3100 to 3300 keV with high resolution (200–300 eV). A well-developed fine structure of the $1/2^-$ analog resonance containing 15 components was found. The strongest component was observed at $E_p = 3219$ keV. Its proton width Γ_p is equal to 500 eV. The $p_{1/2}$ analog state occurs at 10 618 keV in ^{65}Cu. This energy is greater than the neutron separation energy (9908 keV), and therefore the neutron channel is open and the neutron width Γ_n is 410 eV.

An analog of the $f_{5/2}$ ground state of ^{65}Ni was not observed in the (pp) and (pp') reactions, presumably because of the large centrifugal barrier ($l_p = 3$). Analog resonances have not previously been studied in the $(p\gamma)$ reaction. Figure 25 shows the state scheme of the isobaric pair ^{65}Ni and ^{65}Cu.

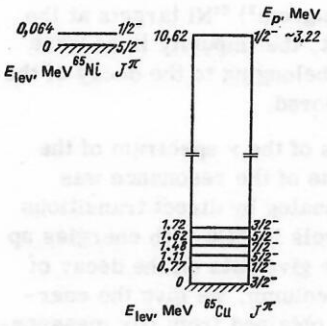

FIG. 25. Scheme of ^{65}Ni levels, their analogs in ^{65}Cu, and low-lying states of ^{65}Cu.

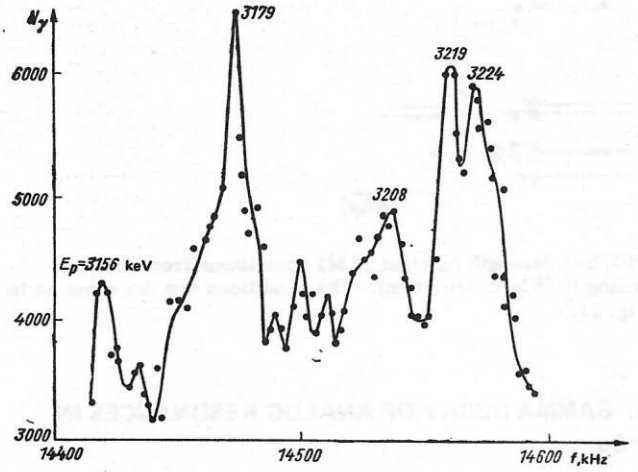

FIG. 26. Excitation function in the reaction ^{64}Ni$(p\gamma)^{65}$Cu in the region of the $p_{1/2}$ analog.

Excitation Function. We measured the excitation function in the reaction ^{64}Ni$(p\gamma)^{65}$Cu for E_p in the interval from 3100 to 3300 keV. The section of the excitation function from 3150 to 3230 keV is shown in Fig. 26.

At E_p = 3208, 3219, 3224 keV, there are peaks corresponding to the strongest components of the fine structure of the $p_{1/2}$ analog observed in Ref. 18. Besides these peaks, there are others at E_p = 3156 and 3179 keV, which were ascribed in Ref. 18 to resonances with $J^\pi = 1/2^+$.

After we had established the position of the analog, we studied the γ-decay of its strongest component with E_p = 3219 keV.

Decay Scheme of the Analog. The γ-decay spectrum of the analog was studied under the conditions already described. Details relating to the determination of the energies, the relative intensities of the γ lines, and the absolute values of the γ widths for transitions from the analog were given above. The measurement and identification of the γ spectra associated with the decay of analogs in ^{65}Cu are more difficult than for ^{59,61,63}Cu because of the higher proton energy at which the analogs are excited in ^{65}Cu. At this energy, there are open neutron channels in reactions that take place on light-element impurities present in the target or in the Faraday cylinder. Therefore, when we identified the γ lines, we compared the spectra measured with thin (10 μg/cm^2) and thick (100 μg/cm^2) ^{64}Ni targets at the given E_p. In the thick target, the impurity lines were much fainter than the lines belonging to the decay of the analog. Such lines were ignored.

As a result of the analysis of the γ spectrum of the resonance, the decay scheme of the resonance was constructed. Decay of the analog by direct transitions leads to population of 24 levels in ^{65}Cu with energies up to 4.3 MeV. In Table XII we give data on the decay of the resonance. In the first column, we give the energies of the populated levels obtained from our measurements. Low-lying levels (up to 1725 keV) were observed in the β-decay of ^{65}Ni. The major part of the highly excited levels observed in our measurements

TABLE XII. Probabilities of direct transitions from the $p_{1/2}$ analog to the ^{65}Cu levels at E_p = 3219 keV, E_{res} = 10618 + 3 keV.

E_{lev}, keV	J^π_{lev}	I_γ, %	Γ_γ, eV	$B(M1)$, μ_0^2
0	3/2$^-$	100	0.15	0.011
770.6±0.5	1/2$^-$	10	0.015	0.0014
1623.8±0.7	5/2$^-$	6	0.009	$E2$
1725.0±0.5	3/2$^-$	76	0.11	0.014
2214.6±1.5	1/2$^-$, 3/2$^-$	14	0.021	0.0030
2331±2	3/2$^-$	15	0.022	0.0032
2644±2	—	17	0.025	0.0042
2656±3	7/2$^-$, 5/2$^-$	10	0.016	—
2867±3	—	58	0.085	0.016
2990±2	—	13	0.019	0.0037
2996±4	—	13	0.019	0.0037
3081±3	—	36	0.053	0.011
3154±3	—	28	0.041	0.0086
3449±3	—	25	0.037	0.0087
3506±3	—	13	0.020	0.0047
3740±3	—	10	0.014	0.0038
3895±3	—	22	0.032	0.0091
3923±3	—	27	0.040	0.012
3958±3	—	16	0.023	0.0068
4057±3	—	20	0.029	0.0090
4084±4	—	17	0.025	0.0076
4117±4	—	19	0.028	0.0088
4183±4	—	31	0.045	0.015
4245±4	—	21	0.030	0.010

was known from various reactions.[52] We have introduced the levels at 3449, 3923, 4057, and 4177 keV for the first time. The quantum numbers J^π for these levels are taken from Ref. 52. For the remaining levels, the J^π values cannot be established sufficiently reliably. In the table we give I_γ, the relative intensities of γ-transitions from the analog to the given level, the partial widths Γ_γ, and $B(M1)$. Since the spin of the resonance at E_p = 3219 keV is assumed to be 1/2, the γ's from the resonance in a transition to any level should be isotropic. We measured the angular distribution for some γ lines from the resonance. The measurements were made at 0, 30, 60, and 90° to the incident proton beam. Within the errors, the angular distributions for the γ-transitions to the ground state of ^{65}Cu and the levels with energies 770.6, 1623, and 1725 keV were isotropic. The $B(M1)$ values were found under the assumption that the transitions are pure $M1$ transitions. Figure 27 shows the strength function of the γ-decay for the main component of the $p_{1/2}$ analog. The errors in the determination of Γ_γ and $B(M1)$ are 30% for strong lines and may be 100% for weak lines.

Analog–Antianalog Transition. It can be assumed that the antianalog for the $p_{1/2}$ analog is the ^{65}Cu level with energy 770.6 keV, which carries the main $p_{1/2}$ single-particle strength: $(2J+1)S(^3\text{He}, d) = 1.5$ (Ref. 52).

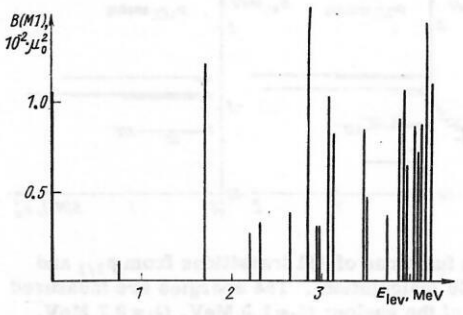

FIG. 27. Values of $B(M1)$ for γ-decay of the $p_{1/2}$ analog in ^{65}Cu (experiment).

TABLE XIII. Analog–antianalog transitions in the Cu isotopes.

Nucleus	T_z	$B(M1)$, μ_0^2 (experiment)	$B(M1)$, μ_0^2 (calculation)	$\frac{B(M1)\text{ exp}}{B(M1)\text{ calc}}$
		$p_{1/2}$ Analog		
^{59}Cu	1/2	0.04	0.13	0.3
^{61}Cu	3/2	0.057	0.090	0.6
^{63}Cu	5/2	0.019	0.077	0.25
^{65}Cu	7/2	0.003	0.058	0.05
		$p_{3/2}$ Analog		
^{61}Cu	3/2	0.24	2.13	0.1
^{63}Cu	5/2	0.0077	1.70	0.004
		$g_{9/2}$ Analog		
^{59}Cu	1/2	1.48	5.1	0.29
^{61}Cu	3/2	0.80	3.6	0.22
^{63}Cu	5/2	0.36	2.8	0.13

The $B(M1)$ value of the analog–antianalog transition is equal to $0.0014 \pm 0.0006\mu_0^2$ for the component with $E_\gamma = 3219$ keV, which, in accordance with Ref. 18, is half the total strength of the $p_{1/2}$ analog. Thus, it can be assumed that the total value of $B(M1)$ for the analog–antianalog transition is $0.003\mu_0^2$; this is much less than the single-particle estimate, which is $0.058\mu_0^2$.

In Table XIII, we give the experimental values of $B(M1)$ for the $p_{1/2}$ analog–antianalog transitions in the Cu isotopes and their single-particle values. A striking feature is the increasing hindrance of the transitions compared with the single-particle estimates with increasing T_z of the nucleus (except ^{59}Cu). A similar tendency is also observed for analog–antianalog transitions of type $p_{3/2}$ and $g_{9/2}$ in the Cu isotopes, the experimental and calculated values of $B(M1)$ for them being also included in Table XIII.

States of Core Polarization Type. It can be seen from Fig. 27 that there is a concentration of the strengths of the transitions from the $p_{1/2}$ analog to the ^{65}Cu levels in the region of energies 3–4 MeV. It was shown in Ref. 4 that the strength functions of the γ transitions from the analogs exhibit a maximum which can be interpreted as strong population of core polarization states. The energies of these states are well predicted by calculations in the shell model with residual interaction.[53] The strength function $M1$ of γ-transitions from the $p_{1/2}$ analog in ^{65}Cu was also calculated. For the values of the parameters chosen as for the nuclei calculated in Ref. 53, we find that the core polarization states must be at a distance of 7 MeV from the analog.

TABLE XIV. Wave functions of states and transition probabilities for the $p_{1/2}$ analog in ^{65}Cu.*

J^π	E_x, MeV	$p_{1/2}(f_{5/2}f_{7/2}^{-1})_{1^+}$	$p_{1/2}(p_{3/2}p_{3/2}^{-1})_{1^+}$	$p_{1/2}(p_{1/2}p_{3/2}^{-1})_{1^+}$	$p_{1/2}$	$B(M1)$, μ_0^2
1/2$^-$	−2.481	0.404	0.618	0.646	0.193	2.704
3/2$^-$	−2.732	0.411	0.627	0.662	—	5.281
1/2$^-$	−6.712	0.355	0.544	−0.759	0.056	0.044
3/2$^-$	−6.718	0.362	0.544	−0.750	—	0.090
3/2$^-$	−7.200	0.837	−0.547	0.000	—	0.421
1/2$^-$	−7.200	0.837	−0.547	0.000	0.001	0.240
1/2$^-$	−9.257	−0.101	−0.152	−0.084	0.980	0.006

*$G_0 = 1.0$ MeV, $G_1 = 1.0$ MeV, $\Delta = 1.8$ MeV, $\varepsilon_{1s_p} = 0.8$ MeV. The energies E_x are measured from the $p_{1/2}$ analog, $E_A = 10.618$ MeV.

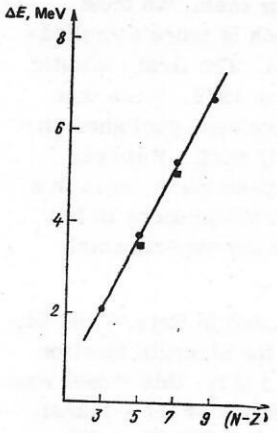

FIG. 28. Dependence of ΔE (the distance from the analog to the core polarization states) on the neutron excess $N-Z$ in the parent nucleus for the Cu isotopes. The filled circles are for the $p_{1/2}$ analogs and the filled squares for the $p_{3/2}$ analogs.

In Table XIV, we give the energies, wave functions, and state population probabilities for the decay of the $p_{1/2}$ analog in ^{65}Cu. It can be seen that the calculation predicts hindrance of the analog–antianalog transition and strong population of states at energy 7.2 MeV from the analog in accordance with the experiment and the systematics on the γ-decay of the analogs. It is of interest to note the experimentally observed dependence in the behavior of the energy spacing ΔE from the analog to the states of the core polarization type in the copper isotopes, namely, ΔE is directly proportional to the neutron excess $N-Z$ of the parent nucleus. This is illustrated in Fig. 28. The dependence of ΔE for the decay of analogs in the Cu isotopes on the neutron excess $N-Z$ of the corresponding Ni isotopes is a straight line with slope 0.75 MeV/(excess nucleon).

6. CALCULATIONS OF PROBABILITIES OF GAMMA TRANSITIONS FROM ANALOGS IN Sc, V, AND Cu ISOTOPES

The experimental data show that the γ-decay of analogs has a number of interesting features due both to the nature of the analog resonances and to the properties of charge-exchange excitations of the proton–neutron hole type with spin 1^+. Analysis of these data leads to numerous questions which can only be answered on the basis of calculations of the strength functions in a model with residual interaction. The main questions are the following: 1) How important are the core polarization states in the γ-decay of the analogs; 2) what is the excitation energy of the core polarization states; 3) how does an admixture of core polarization states in the antianalog affect the probability of analog–antianalog transitions; 4) how strongly do the strength functions differ for Gamow–Teller β-transitions and $M1$ γ-transitions from analogs?

Almost all these questions arose during the analysis of the results of our measurements on the γ-decay of

analogs in ^{51}V (Ref. 5). To answer them, we must make calculations in a model which is more complicated than the single-particle model. The first realistic calculations were made by Ikeda in 1969. Since that time, many experimental data have been published on nuclei in the $f_{7/2}$ shell and the $2p1f$ shell. However, systematic calculations have not been made, even in a simple model. The need for such calculations is felt when one attempts to systematize the experimental data.

We used the model first formulated in Refs. 8 and 54, in which it was used to calculate the strength function of Gamow–Teller β-transitions. Later, this model was used to calculate the strength function of $M1$ γ-transitions from analogs in ^{51}V (Ref. 5) and ^{49}Sc (Ref. 55).

We obtained compact expressions for the matrix elements of the interaction and for the transition probabilities. Below, we formulate the model that we used, we give the corresponding expressions for the matrix elements and the transition probabilities, and we describe the results of the calculations.

To treat charge-exchange excitations of particle–hole type, we proceed from the Hamiltonian H_0 of the independent-particle shell model and a residual interaction of a specific type:

$$\mathcal{H} = \mathcal{H}_0 + \mathcal{H}_I. \tag{2}$$

The independent-particle Hamiltonian contains the terms

$$\mathcal{H}_0 = \mathcal{H}_0' + \mathcal{H}_{ls} + \mathcal{H}_c, \tag{3}$$

where $\mathcal{H}_0' = \sum_i [T_i + V(r_i)]$ is the kinetic and potential energy of the particles, $\mathcal{H}_{ls} = \sum_i 1/2 V_{ls} l_i \sigma_i$ is the spin–orbit interaction, and $\mathcal{H}_c = \sum_{ij}(1+\tau_{zi}/2)v_c(r_{ij})$ is the Coulomb interaction.

The residual interaction can be written in the form

$$\mathcal{H}_I = \mathcal{H}_\tau + \mathcal{H}_{\sigma\tau} + \mathcal{H}_\sigma = \frac{G_0}{2}\sum_{i>j}\tau_i\tau_j + \frac{G_1}{2}\sum_{i>j}\tau_i\tau_j\sigma_i\sigma_j + \frac{G_2}{2}\sum_{i>j}\sigma_i\sigma_j. \tag{4}$$

We shall use an interaction of long-range type in the form of multipole forces. The radial integrals are replaced by a constant K. Only the isospin part of the interaction (4) is considered.

Basis States and their Energies. As basis functions, we choose the single-particle and particle–hole configurations that are the most important when one is considering the γ-decay of analogs. Since we are studying the decay of well-defined single-proton analogs, the wave functions of the corresponding parent states can be assumed to be single-neutron states:

$$\Psi^{PS} = |j_{n_1}\rangle = a^+_{j_{n_1}}|\hat{0}\rangle, \tag{5}$$

where $|\hat{0}\rangle$ is the wave function of the target nucleus. The basis functions include configurations formed from (5) by applying the operator Y_-:

$$\Psi_i = Y_-|j_{n_1}\rangle. \tag{6}$$

These states are eigenfunctions of the single-particle Hamiltonian $\tilde{\mathcal{H}}_0$:

$$\tilde{\mathcal{H}}_0\Psi_i = E_i\Psi_i.$$

The single-particle configurations include the single-proton state

$$\Psi_1 = |j_{p_1}\rangle \tag{7}$$

corresponding to (5) and its spin–orbit partner

$$\Psi_1' = |j_{p_2}\rangle. \tag{8}$$

In what follows, a prime on the function Ψ means that the odd particle occupies the second term of the spin–orbit doublet.

The particle–hole configurations have the form

$$\Psi_2 = |[j_{n_1}(j_p j_{n^{-1}})_I]\,J\rangle = \sum_{\substack{m_{n_1} m \\ m_p m_n}} \langle j_{n_1} m_{n_1} I m | J M\rangle \langle j_p m_p j_n - m_n | I m\rangle \times (-)^{j_n - m_n} a^+_{j_{n_1} m_{n_1}} a^+_{j_p m_p} a_{j_n m_n}|\hat{0}\rangle. \tag{9}$$

The configuration Ψ_2' is expressed in the same way as (9), containing instead of j_{n_1} a particle on the level j_{n_2}, which is the spin–orbit partner of j_{n_1}. In the functions Ψ_2 and Ψ_2', the proton j_p and the neutron hole $j_{n^{-1}}$ are in the same state.

The functions Ψ_3 and Ψ_3' are expressed in the same way as (9) but contain configurations in which the proton j_p and the neutron hole $j_{n^{-1}}$ are in different states forming a spin–orbit doublet. In numerical calculations, we took into account particle–hole excitations with only $I^\pi = 1^+$. As will be shown in what follows, these excitations play the main role in β-decay and $M1$ γ-decay of the analogs.

The particle and particle–hole configurations for the considered nuclei take into account the shells $f_{7/2}$, $p_{3/2}$, $p_{1/2}$, $f_{5/2}$, and $g_{9/2}$.

The energies E_i of the basis states, measured from the energy of the analog state, are expressed as

$$\left.\begin{aligned} &E_1 = -2T_0G_0; \quad E_1' = -2T_0G_0 + \varepsilon_{p(ls)};\\ &E_2 = -2T_0G_0 + \Delta; \quad E_2' = -2T_0G_0 + \Delta + \varepsilon_{n(ls)};\\ &E_3 = -2T_0G_0 + \Delta + \varepsilon_{np(ls)};\\ &E_3' = -2T_0G_0 + \Delta + \varepsilon_{n(ls)} + \varepsilon_{np(ls)}. \end{aligned}\right\} \tag{10}$$

In these expressions, T_0 is the isospin of the analog, Δ is the pairing energy of the excess neutrons, $\varepsilon_{n(ls)}$ and $\varepsilon_{p(ls)}$ are the spin–orbit splitting of the neutron or proton states, and $\varepsilon_{np(ls)}$ is the difference between the energies of the proton state $j_p = l - 1/2$ and the corresponding neutron state $j_n = l + 1/2$.

The states Ψ_2 and Ψ_2' have definite isospin, this being smaller by unity than the isospin of the analog state.

The configurations Ψ_1, Ψ_1' and Ψ_3, Ψ_3' do not have definite isospin. However, for the solution of problems relating to isospin it is convenient to use a basis that has definite isospin. This can be particularly important in cases when a strongly restricted basis is used.

Parameters of the Theory. The parameters which can be specified in calculations are divided into two groups: the interaction parameters G_0 and G_1 and the parameters which determine the average field.

The constant G_0, which determines the symmetry energy, is fairly well known. It is determined from the analysis of quasielastic scattering, from isospin splitting of single-particle states, and from other experiments.[3] The value of this constant fluctuates rather

strongly from nucleus to nucleus, but on the average one can take its value to be $G_0 = 50/A$ MeV.

The constant G_1, which determines the strength of the spin–isospin interaction, is not known exactly. In contrast to G_0, for G_1 there is no physically measured quantity directly related to G_1. However, one can establish limits within which G_1 can vary.[8] One of the extreme values for G_1 is realized when supermultiplet symmetry is observed, as, for example, in light nuclei. Then

$$G_0 = G_1 = G_2; \quad V_{1s}(r) = \mathscr{H}_c = 0; \quad [\mathscr{H}_I, T] = 0;$$
$$[\mathscr{H}_I, Y] = 0; \quad [\mathscr{H}_I, S] = 0;$$
$$\mathscr{H}_I = G_0/2 \sum_{i>j} (1 + \tau_i\tau_j)(1 + \sigma_i\sigma_j) + \text{const}.$$

In light nuclei, cases are known when a splitting is observed of states with $T = 0$, $J = 1^+$ and $T = 1$, $J = 0^+$ (2–3 MeV). From this one can estimate the ratios of the constants to be $G_0 : G_1 : G_2 = 3:2:1$. In other cases, intermediate estimates are obtained. Thus, for the ratio G_1/G_0 we have the limits $2/3 \leq G_1/G_0 \leq 1$. Analysis of the (pn) reaction indicates that G_1 is close to the limit $(2/3)G_0$ (Ref. 56).

The parameters that determine the average field are the magnitude of the spin–orbit splitting and the pairing energy Δ. In the numerical calculations, no distinction was made between the spin–orbit splittings for the neutrons and protons.

In the calculations reported here, the spin–orbit splittings were taken from the experimental data for the parent nucleus. This choice automatically leads to the correct position of the analog states. Our calculations were made with several values of Δ from 0 to 2 MeV. All the parameters were varied within the limits allowed by the experimental data and theoretical arguments. The variation was performed to determine the sensitivity of the results to the values of the parameters.

Matrix Elements of the Interaction V. To calculate the matrix of the Hamiltonian H and then diagonalize it, we must calculate the following matrix elements:

a) diagonal and nondiagonal matrix elements of the type

$$\langle \Psi_{3i} | V | \Psi_{3k} \rangle, \ \langle \Psi_{3i} | V | \Psi'_{3k} \rangle, \ \langle \Psi'_{3i} | V | \Psi'_{3k} \rangle,$$
$$\langle \Psi_{2i} | V | \Psi_{2k} \rangle, \ \langle \Psi_{2i} | V | \Psi'_{2k} \rangle, \ \langle \Psi'_{2i} | V | \Psi'_{2k} \rangle;$$

b) nondiagonal matrix elements of the type

$$\langle \Psi_{2i} | V | \Psi_{1k} \rangle, \ \langle \Psi'_{2i} | V | \Psi_{1k} \rangle, \ \langle \Psi'_{2i} | V | \Psi'_{1k} \rangle;$$

c) diagonal matrix elements of the type

$$\langle \Psi_{1i} | V | \Psi_{1k} \rangle, \ \langle \Psi'_{1i} | V | \Psi'_{1k} \rangle.$$

For each case, analytic expressions can be obtained.

Using the expression (9) and summing over the magnetic quantum numbers, we obtained the following expressions for the matrix elements of the interaction:

$$\langle [j'_{n_1}, (p'n'^{-1})_{I'}] J' | V | [j_{n_1}(p, n^{-1})_I] J \rangle$$
$$= 1/3 \langle j'_p \| \sigma \| j'_n \rangle \langle j_p \| \sigma \| j_n \rangle \delta_{j'_{n_1} j_{n_1}} \delta_{I, 1} \delta_{I', 1} \delta_{J, J'}$$
$$+ \sqrt{(2J+1)(2I'+1)} \begin{Bmatrix} J & j'_{n_1} & I' \\ j_{n_1} & 1 & j'_p \\ I & j_p & j_n \end{Bmatrix} \langle j'_p \| \sigma \| j_{n_1} \rangle$$
$$\times \langle j_p \| \sigma \| j'_{n_1} \rangle \delta_{j'_n j_n} \delta_{JJ'}; \qquad (11)$$

$$\langle [j'_{n_1}, (p'n'^{-1})_{I'}] J' | V | j_{p_1} \rangle$$
$$= \frac{1}{\sqrt{3(2j_p+1)}} \langle j'_p \| \sigma \| j'_n \rangle \langle j_{p_1} \| \sigma \| j'_{n_1} \rangle \delta_{I', 1} \delta_{J', j_{p_1}}; \qquad (12)$$

$$\langle j'_{p_1} | V | j_{p_1} \rangle = 0. \qquad (13)$$

In the numerical calculations, the second term in the expression (11) was not taken into account.

The expressions (11)–(13) were obtained for the case when the protons and neutrons (apart from the odd neutron in the parent nucleus) completely occupy neighboring shells, i.e., when the excess neutrons completely populate the shell j_n, and the protons completely populate the preceding shell. The proton levels corresponding to the neutron shell j_n are completely free. In other cases, when the neutrons do not completely occupy a shell or when there are several protons on levels corresponding to the neutron shell j_n, corresponding occupation coefficients u_p and v_n are introduced. Then each matrix element of the type $\langle j_p \| \sigma \| j_n \rangle$ is associated with a certain quantity $\langle j_p \| \sigma \| j_n \rangle u_p v_n$

$$\langle j_p \| \sigma \| j_n \rangle \to \langle j_p \| \sigma \| j_n \rangle u_p v_n,$$

where $v_n = \sqrt{n_{j_n}/(2j_n+1)}$ and $u_p = \sqrt{1 - n_{j_p}/(2j_p+1)}$, n_{j_n} is the number of neutrons on level j_n, and n_{j_p} is the number of protons on level j_p.

To calculate the matrix elements of the interaction, we must know the quantities $\langle l_j \| \sigma \| l_{j'} \rangle$:

$$\langle l_j \| \sigma \| \ l_{j'} \rangle = (-)^{l+1/2-j'} \sqrt{(2j+1)(2j'+1)} \sqrt{2 - \delta_{jj'}}$$
$$\times \left[\frac{(j+j'+2)!\,(j'+l-1/2)!\,(j+l-1/2)!}{(j+j'-1)!\,(j'+l+3/2)!\,(j+l+3/2)!} \right]^{1/2}. \qquad (14)$$

We also have the relation

$$\langle j \| \sigma \| j' \rangle = (-)^{j-j'} \langle j' \| \sigma \| j \rangle. \qquad (15)$$

The matrix of the Hamiltonian was diagonalized numerically, and for each spin value J we then obtained a set of wave functions

$$\Psi_i(J, M) = \sum_k c^J_{ik} \Psi_k. \qquad (16)$$

Transition Probabilities. The reduced probability of an $M1$ γ-transition from the analog to the state $\Psi_f(J, M)$ can be expressed as follows:

$$B(M1, \text{an.} \to JM) =$$
$$= \frac{1}{2J_i+1} | \langle \Psi^{J_f}_{T_0, T_0} \| F^\lambda (k\tau = 1) \| \Psi^{\text{AS}}_{T_0+1, T_0} \rangle. \qquad (17)$$

The γ-decay of the analogs can be regarded as a charge-exchange process:

$$\langle \Psi_{T_0, T_0} \| \sum_i m^\gamma_l (x_i) t_z(i) \| \Psi^{\text{AS}}_{T_0+1, T_0} \rangle$$
$$= \frac{1}{\sqrt{2(T_0+1)}} \langle \Psi_{T_0, T_0} \| \sum_i m^\gamma_l (x_i) [T_-, t_z(i)] \| \Psi^{\text{PS}}_{T_0+1, T_0+1} \rangle$$
$$= \frac{1}{\sqrt{2(T_0+1)}} \langle \Psi_{T_0, T_0} \| \sum_i m^\gamma_l (x_i) t_-(i) \| \Psi^{\text{PS}}_{T_0+1, T_0+1} \rangle. \qquad (18)$$

The probability of β-transition from the parent state $\Psi^{\text{PS}}_{T_0+1, T_0+1}$ to the state Ψ_{T_0, T_0} is determined by a reduced matrix element of the type

$$\langle \Psi_{T_0, T_0} \| \sum_i m^\beta_l (x_i) \tau_-(i) \| \Psi^{\text{PS}}_{T_0+1, T_0+1} \rangle. \qquad (19)$$

Using now (18), we can write the reduced probability of transition from the analog in the form

$$B(M1, \text{an.} \to JM) = \frac{3}{4\pi}\mu_-^2 \frac{1}{2T_0} \sum_M |\langle \Psi_i(JM) | m(M1) j_{n_1} m_{n_1}\rangle|^2 = \Big| \sum_k c_{ik}^J B^{1/2}(M1, j_{n_1} \to \Psi_k)\Big|^2, \quad (20)$$

where $\mu_- = \mu_p - \mu_n = 4.71$ is the difference between the proton and neutron magnetic moments, T_0 is the isospin of the analog, and

$$m(M1) = \sum_i \left(\sigma_i + \frac{g_l}{\mu_-} l_i\right) t_-(i). \quad (21)$$

Using the relation between ft for the β-transition and the value of $B(M1, \sigma)$ for the transition from the analog, we can obtain the expression

$$B(M1, \sigma) = B(M1, \sigma; \Psi^{PS} \to \Psi_i(JM)) = \frac{3}{4\pi}\mu_-^2 \sum_M |\langle \Psi_i(JM) | m(M1, \sigma) | j_{n_1} m_{n_1}\rangle|^2 = \Big| \sum_k c_{ik}^J B^{1/2}(M1, \sigma; j_{n_1} \to \Psi_k)|^2, \quad (22)$$

where $m(M1, \sigma) = Y_- = \sum_i \sigma_i \tau_-(i)$.

The transition probabilities to the unperturbed states can be expressed in the form

$$B(M1, \sigma; j_{n_1} \to \Psi_1) = \frac{3}{4\pi}\left(\frac{e\hbar}{2mc}\right)^2 \mu_-^2 \times \frac{1}{(2j_{n_1}+1)} \langle j'_{p_1} \| \sigma \| j_{n_1}\rangle; \quad (23)$$

$$B(M1, \sigma; j_{n_1} \to \Psi_2) = B(M1, \sigma; j_{n_1} \to \Psi_3) = \frac{3}{4\pi}\left(\frac{e\hbar}{2mc}\right)^2 \mu_-^2 \frac{2I'+1}{3(2j_{n_1}+1)} \langle j'_p \| \sigma \| j'_n\rangle^2 \delta_{j'_{n_1} j_{n_1}}. \quad (24)$$

The reduced probability for γ-transition is calculated as follows:

$$B(M1; j_{n_1} \to \Psi_i) = B(M1, \sigma; j_{n_1} \to \Psi_i)(1 + g_l k/\mu_-)^2, \quad (25)$$

where

$$k = \begin{cases} +l & \text{for transitions } j_> \to j_>; \\ -1/2 & \text{for transitions } j_> \to j_< \text{ or } j_< \to j_>; \\ -(l+1) & \text{for transitions } j_< \to j_<. \end{cases}$$

Numerical Calculations. Numerical calculations were made for the following analog states[53]:

1) $p_{3/2}$ in ^{43}Sc, ^{45}Sc, ^{47}Sc, ^{49}Sc, ^{49}V, ^{47}V, ^{51}V;
2) $p_{3/2}$ in ^{59}Cu, ^{61}Cu, ^{63}Cu;
3) $p_{1/2}$ in ^{59}Cu, ^{61}Cu, ^{63}Cu;
4) $f_{5/2}$ in ^{61}Cu and ^{63}Cu;
5) $g_{9/2}$ in ^{59}Cu, ^{61}Cu, ^{63}Cu.

Experimental data are available for all the studied cases.

We obtained data for the decay of the $p_{3/2}$ analogs in ^{43}Sc and ^{51}V, the $p_{3/2}$ and $p_{1/3}$ analogs in ^{59}Cu, ^{61}Cu, ^{63}Cu, and the $f_{5/2}$ analogs in ^{61}Cu and ^{63}Cu. The results for the remaining analogs were obtained by other groups.

TABLE XV. Wave functions and transition probabilities for $g_{9/2}$ analogs in ^{63}Cu.*

J^π	E_x, MeV	$g_{9/2}(f_{5/2}f_{5/2}^{-1})_{1^+}$	$g_{9/2}(p_{3/2}p_{3/2}^{-1})_{1^+}$	$g_{9/2}(p_{1/2}p_{3/2}^{-1})_{1^+}$	$g_{9/2}$	$B(M1)$, μ_0^2
9/2+	−3.600	0.566	0.590	0.482	0.315	2.59
11/2+	−3.976	0.582	0.633	0.510	—	1.49
7/2+	−3.976	0.582	0.633	0.510	—	1.01
9/2+	−5.990	−0.694	0.716	−0.010	−0.079	0.32
11/2−	−6.001	0.736	−0.677	0.000	—	0.53
7/2+	−6.001	0.736	−0.677	0.000	—	0.35
9/2+	−6.143	−0.367	−0.346	0.863	−0.015	0.01
11/2+	−6.144	−0.345	−0.376	0.860	—	0.01
7/2+	−6.144	−0.345	−0.376	0.860	—	0.01
9/2+	−7.383	−0.252	−0.142	−1.148	0.946	1.96

*$G_0 = 1.0$ MeV, $G_1 = 0.70$ MeV, $\Delta = 1.0$ MeV, $\varepsilon_{1sp} = -0.2$ MeV. The energies E_x are measured from the analog.

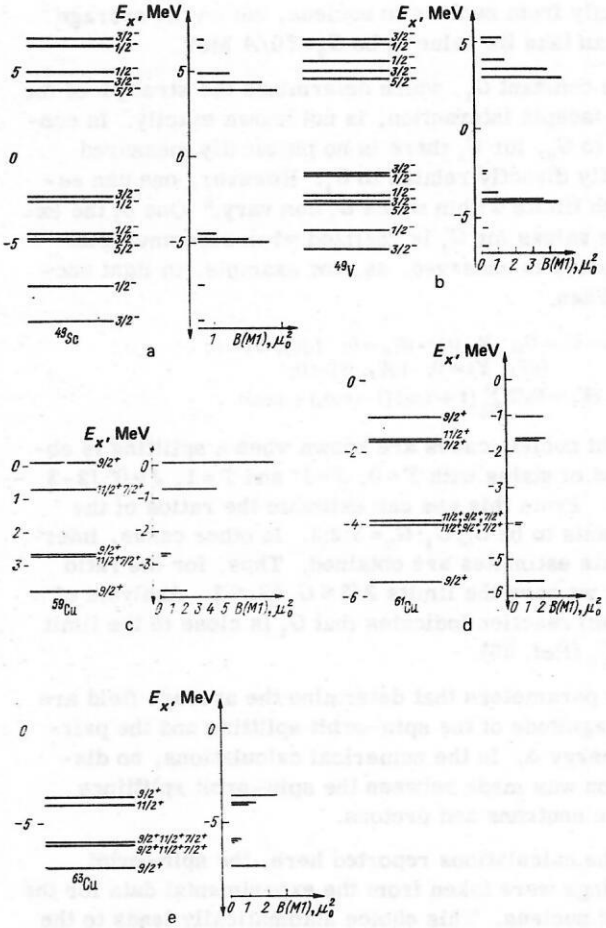

FIG. 29. Strength function of $M1$ transitions from the $p_{3/2}$ analog in ^{49}Sc (a), ^{49}V (b), and from the $g_{9/2}$ analog in ^{59}Cu (c), ^{61}Cu (d), and ^{63}Cu (e) (calculation). The energies are measured from the position of the analog. a) $G_0 = 0.92$ MeV, $G_1 = 0.81$ MeV, $\Delta = 2.00$ MeV, $\varepsilon_{1sp} = 2.5$ MeV, $\varepsilon_{1sf} = 5.00$ MeV; b) 1.00, 0.90, 0.00, 1.60, 4.00; c) 1.00, 1.00, 0.00, 0.52; d) 1.00, 0.90, 1.00, 0.2; e) 1.00, 0.70, 1.00, 0.2.

As a result of the calculations, we can follow the behavior of the strength functions of $M1$ transitions from the same analogs in different isotopes of one element. Another possibility is to study the behavior of the decay of different analogs in the same nucleus (copper isotopes).

In each of the five groups, the qualitative nature of the strength function of $M1$ transitions from analogs is the same. The results for some nuclei have already been given. Here, we present the results for the calculations of the other nuclei. In Fig. 29, we show the strength functions of $M1$ γ-transitions from the $p_{3/2}$ analogs in ^{49}Sc and ^{49}V and from the $g_{9/2}$ analogs in ^{59}Cu, ^{61}Cu, ^{63}Cu. In Table XV, we give the wave functions of the ^{63}Cu states associated with the $g_{9/2}$ analog. The wave functions in other cases have a qualitatively similar nature in each group.

7. ANALYSIS OF THE RESULTS

In all cases, the lowest states are the states with the largest contribution of the corresponding single-particle component. These states are called antianalog states. All the remaining components, whose contribution may be fairly large, have a counter effect when added to the single-particle component, reducing the probability of the analog–antianalog transition.

At excitation energies a few MeV above the antianalog there is a group of states in whose wave functions the main component is a particle–hole configuration in which the proton and the neutron hole are on the same level. Such states are called states of core polarization type. Note that in all nuclei this group is localized in a relatively small range of excitation energies and is strongly populated by the γ-decay of the analog.

The greater part of the strength of the $M1$ transitions associated with the analog is concentrated on states near or above the analog. These states from the so-called Gamow–Teller giant resonance. The main component in the wave functions of these states is a particle–hole state $[\Psi_3]$ of spin-flip type. The amplitudes of the various components in the functions of these states have the same sign. These states can be regarded as collective states of particle–hole type, and their appearance in the present model is not fortuitous, since the model is a special case of the "schematic model."[57,58]

Beta and Gamma Analog Transitions. The distributions of $B(M1)$ for γ-transitions from the analog and $B(M1,\sigma)$ for β-transitions from the corresponding parent state exhibit a common feature, namely, concentration of the transition probability on levels above or near the analog resonance. The major part (up to 90%) of the strength of the transitions is concentrated on the levels which form the Gamow–Teller giant resonance. The difference between the strength functions for the $M1$ γ- and β-transitions is greatest for population of core polarization states. Beta-transitions populate such states comparatively weakly, whereas in the β-decay of analogs the core polarization states are observed almost as strongly as the Gamow–Teller giant resonance. It is possible that this effect is due to the model form of the chosen interaction, which ensures a large concentration of β-transitions. For the transitions to the antianalog states, the probabilities of β- and γ-transitions are comparable in magnitude.

TABLE XVI. Analog–antianalog transitions and population of core polarization states.

Nucleus	Analog	$B(M1)$, μ_0^2 Analog–antianalog (calculation)	$B(M1)$, μ_0^2 Analog–antianalog (single-particle calculation)	$B(M1)$, μ_0 Analog–antianalog (experiment) (Ref. 4)	$B(M1)$, μ_0^2 Core polarization (calculation)	$B(M1)$, μ_0^2 Core polarization (experiment) (Ref. 4)
^{43}Sc	$p_{3/2}$	0.72	2.85	0.012	11.3	0.17
^{45}Sc	$p_{3/2}$	0.37	2.06	—	9.6	2.1
^{47}Sc	$p_{3/2}$	0.31	1.58	0.012	8.4	0,3
^{49}Sc	$p_{3/2}$	0.24	1.27	0.002	8.4	5.2
^{47}V	$p_{3/2}$	0.64	2.85	0.017	11.7	0.7
^{49}V	$p_{3/2}$	0.48	2.06	0.032	9.2	1.2
^{51}V	$p_{3/2}$	0.30	1.53	0.015	9.2	1.3
^{59}Cu	$g_{9/2}$	3.13	4.92	1.48	1.3	—
^{61}Cu	$g_{9/2}$	2.08	3.53	0.80	1.3	—
^{63}Cu	$g_{9/2}$	1.90	2.70	0.36	1.2	—
^{61}Cu	$p_{3/2}$	0.87	2.06	0.24	1.3	1.0
^{63}Cu	$p_{3/2}$	0.69	1.58	0.0077	1.3	0.3
^{59}Cu	$p_{1/2}$	0.001	0.13	0.04	3.0	0.8
^{61}Cu	$p_{1/2}$	0.001	0.09	0.057	1.3	0.5
^{63}Cu	$p_{1/2}$	0.001	0.07	0.019	1.3	0.3
^{61}Cu	$f_{5/2}$	0.09	0.014	0.0047	1.1	0.1
^{63}Cu	$f_{5/2}$	0.05	0.010	0.019	1.3	0.1
^{65}Cu	$p_{1/2}$	0.006	0.06	~0.0014	0.63	0.1

Analog–Antianalog Transitions. The calculated $B(M1)$ values for the analog–antianalog transitions are given in Table XVI, in which we also give the theoretical and experimental values of $B(M1)$ for the single-particle transitions. Note that the probabilities of analog–antianalog transitions calculated in the present model agree better with the experiment than the calculations using the single-particle model. It is predicted that the transition probabilities for $p_{3/2}$ analogs will be suppressed in the Sc and V isotopes but that there will be the single-particle value of the transitions for the $g_{9/2}$ analogs in the Cu isotopes. For the $p_{3/2}$ analogs in ^{61,63}Cu, the predicted values of $B(M1)$ for the analog–antianalog transitions are somewhat less than the single-particle estimate. Thus, the qualitative dependence of the analog–antianalog transition probabilities on the quantum numbers of the analogs and the considered nucleus is correctly predicted by the model. However, in the quantitative respect there are discrepancies. The suppression of the analog–antianalog transitions for $p_{3/2}$ states in Sc and V is much smaller than is observed experimentally. Variation of the constant C_1 within wide limits does not lead to agreement with the experiment. The same discrepancy is observed for the $p_{3/2}$ analogs in ^{63}Cu. The transition probabilities for the $g_{9/2}$ and $p_{3/2}$ analogs in ^{61}Cu are described fairly well.

Core Polarization. As we noted earlier, in each nucleus there is a group of states in the wave functions of which components of the type Ψ_2 are added coherently. If only these components were taken into account, we should obtain a collective state of the type

$$j_{n_1}(j_p j_{n-1})_{1\Phi},\ j_p = j_{n-1}.$$

Allowance for spin-flip states leads to mixing of two configurations with transfer of the transition intensity to the upper state forming the Gamow–Teller giant resonance. The energy position (with respect to the analog) of the core polarization states depends weakly on the constant G_1. The strongest dependence observed is that on Δ: $E_A - E_m = E_0 - \Delta$, where E_0 does not depend on Δ. The levels forming the core polarization states have spins $j_{n_1}-1$, j_{n_1}, $j_{n_1}+1$. In real nuclei, the configurations corresponding to states of core polarization type are distributed over the real levels of the nucleus and a structure of the giant resonance type is manifested.

For reasonable values of the parameters, the calculated mean excitation energies of the core polarization states (measured from the ground states) for the $p_{3/2}$ analogs are as follows: 3.8 MeV for ^{43}Sc, 5.0 MeV for ^{45}Sc, 6.7 MeV for ^{47}Sc, 6.8 MeV for ^{49}Sc, 4.7 MeV for ^{47}V, 3.8 MeV for ^{49}V, 4.8 MeV for ^{51}V, 2.8 MeV for ^{61}Cu, 3.7 MeV for ^{63}Cu, 2.9 MeV for $f_{5/2}$ in ^{61}Cu, 3.9 MeV for ^{63}Cu, 4.4 MeV for $g_{9/12}$ in ^{59}Cu, 4.1 MeV for ^{61}Cu, and 3.7 MeV for ^{63}Cu.

A characteristic feature of the experimental data on the γ-decay of analogs in the Sc, V, Cu isotopes is the strong population of groups of states a few MeV above the antianalog. The experimental excitation energies of these states agree well with the calculated position of the core polarization states.

The experimental data make it possible to determine the total value of $B(M1)$ for the transitions to these states and to compare it with the calculated value of $B(M1)$ for transitions to core polarization states. In Table XVI, we give the theoretical values and the corresponding experimental data. Note that the calculations give the correct ratio of the $B(M1)$ value of the transitions to the antianalog and the core polarization states for different nuclei. For the Sc and V isotopes, it is predicted that core polarization states will be predominantly populated; for the Cu isotopes ($g_{9/2}$ analogs), the antianalogs. For other analogs in the Cu isotopes correct relations are also obtained. The absolute values of $B(M1)$ for transitions to core polarization states are predicted to be larger than the experimental values.

For some nuclei, this difference is small (by a few times), but traces of strong deviation are encountered. For Cu isotopes, the agreement can be regarded as good. For the $g_{9/2}$ analogs, no data are available on the population of core polarization states, which can be attributed to the experimental difficulties.

We mention an interesting property of core polarization states revealed by the calculations. To good accuracy, the difference between the energies of the analog and the corresponding core polarization state does not depend on the quantum numbers of the odd particle. Such an effect had been observed earlier experimentally.

Gamow–Teller Resonance. In all the nuclei, the group of states near or above the antianalog carries the main strength of the transition. These states form the Gamow–Teller resonance. For β-transitions, more than 90% of the total strength can be concentrated in the region of the Gamow–Teller resonance. In the case of $M1$ γ-transitions this fraction is smaller and may be reduced to 50%.

The present model correctly describes the main qualitative features of the γ-decay of analogs. It predicts the correct relationship between the intensities of the analog–antianalog transitions for different nuclei and different analogs, and the energies of the core polarization states agree well with the experimental values found for the position of the maximum in the strength functions of γ-transitions from the analogs.

However, for the absolute values of the transition intensities a discrepancy between the calculated and experimental values is observed. The probabilities for strong transitions give the best agreement. For the probability of the analog–antianalog transitions in Sc and V the calculations give less hindrance than is observed experimentally.

[1]J. D. Anderson and C. Wong, Phys. Rev. Lett. 7, 250 (1961).
[2]J. D. Fox, C. F. Moore, and D. Robson, Phys. Rev. Lett. 12, 198 (1964).
[3]Yu. V. Naumov and O. E. Kraft, Izospin v yadernoĭ fizike (Isospin in Nuclear Physics), Nauka, Moscow–Leningrad (1972).
[4]Yu. V. Naumov and O. E. Kraft, Fiz. Elem. Chastits At. Yadra 6, 892 (1975) [Sov. J. Part. Nucl. 6, 361 (1975)]; Materialy XI zimneĭ shkoly LIYaF (Proc. Eleventh Winter School at the Leningrad Institute of Nuclear Physics), Leningrad (1976), p. 33; Izv. Akad. Nauk SSSR Ser. Fiz. 39, 1656 (1975); Yu. V. Naumov, Izv. Akad. Nauk SSSR Ser. Fiz. 38, 1617 (1974).
[5]C. Gaarde *et al.*, Nucl. Phys. A143, 497 (1970); H. V. Klapdor, Phys. Lett. B35, 405 (1971).
[6]B. Mottelson, Usp. Fiz. Nauk 120, 563 (1976).
[7]V. G. Solov'ev, Teoriya slozhnykh yader, Nauka, Moscow (1971) (English translation: Theory of Complex Nuclei, Pergamon Press, Oxford (1976)).
[8]T. Fujita and K. Ikeda, Nucl. Phys. 67, 145 (1975).
[9]S. I. Gabrakov, A. A. Kuliev, and N. I. Pyatov, Phys. Lett. B36, 275 (1971).
[10]Yu. V. Gaponov and Yu. S. Lyutostanskiĭ, Yad. Fiz. 19, 62 (1974) [Sov. J. Nucl. Phys. 19, 33 (1974)].
[11]B. L. Birbrair, Yad. Fiz. 5, 1198 (1967) [Sov. J. Nucl. Phys. 5, 857 (1967)].
[12]D. F. Zaretskiĭ and M. G. Urin, Yad. Fiz. 8, 731 (1968) [Sov. J. Nucl. Phys. 8, 425 (1969)].
[13]V. P. Aleshin, Izv. Akad. Nauk SSSR Ser. Fiz. 37, 1959 (1973).
[14]T. Fujita, Y. Futami, and K. Ikeda, Prog. Theor. Phys. 38, 107 (1967).
[15]G. C. Morrison and J. P. Schiffer in: Isobaric Spin in Nuclear Physics (Eds. J. D. Fox and D. Robson), Academic Press, London (1966), p. 748.
[16]J. W. Butler and C. R. Gossett, Phys. Rev. 108, 1473 (1957).
[17]J. H. Carver and G. A. Jones, Nucl. Phys. 19, 184 (1960).
[18]J. C. Browne *et al.*, Nucl. Phys. 153, 481 (1970).
[19]J. P. Trentelman *et al.*, Nucl. Phys. A246, 457 (1975).
[20]O. E. Kraft *et al.*, Izv. Akad. Nauk SSSR Ser. Fiz. 41, 82 (1977).
[21]O. E. Kraft, Yu. V. Naumov, and I. V. Sizov, Izv. Akad. Nauk SSSR Ser. Fiz. 39, 70 (1975).
[22]S. Galès *et al.*, Nucl. Phys. A268, 257 (1976).
[23]O. E. Kraft *et al.*, Izv. Akad. Nauk SSSR Ser. Fiz. 40, 1182 (1976).
[24]D. Van Patter, F. Rauch, and B. Seim, Nucl. Phys. A204, 172 (1973).
[25]E. R. Cosman *et al.*, Phys. Rev. 163, 1134 (1967).
[26]D. J. Pullen and B. Rosner, Phys. Rev. 170, 1034 (1968).
[27]C. R. Gossett and L. S. August, Phys. Rev. B 137, 381 (1965).
[28]B. Rosner, C. Holbrow, and D. Pullen, in: Isobaric Spin in Nuclear Physics (Eds. J. D. Fox and D. Robson), Academic Press, London (1966).
[29]E. J. Hoffman, D. G. Sarantites, and N. H. Lu, Nucl. Phys. A173, 146 (1971).
[30]Nucl. Data B 2, No. 5 (1968).
[31]O. E. Kraft, Yu. V. Naumov, and I. V. Sizov, Soobshcheniya (Communications) R15-8201, R15-8202, JINR, Dubna (1974); Yad. Fiz. 20, 1081 (1974); 21, 919 (1975) [Sov. J. Nucl. Phys. 20, 567 (1975); 21, 472 (1975)].
[32]D. Cline and P. Lesar, Nucl. Instrum. Methods 82, 291 (1970).
[33]O. E. Kraft *et al.*, Soobshchenie (Communication) R15-7072, JINR, Dubna (1973).
[34]T. R. Aufinsen *et al.*, Nucl. Phys. A157, 561 (1970).
[35]R. H. Fulmer and A. L. McCarthy, Phys. Rev. 131, 2133 (1963).
[36]V. F. Litvin *et al.*, Nucl. Phys. A184, 105 (1972).
[37]E. Takasaki, J. Phys. Soc. Jpn. 32, 569 (1972).
[38]I. D. Lopatko *et al.*, Izv. Akad. Nauk SSSR Ser. Fiz. 35, 1707 (1971).
[39]B. Ya. Guzhovskiĭ *et al.*, Izv. Akad. Nauk SSSR Ser. Fiz. 33, 129 (1969).
[40]O. E. Kraft *et al.*, Tezisy dokladov na XXIV soveshchanii po yadernoĭ spektroskopii i strukture yadra (Abstracts of Pa-

pers at the 24th Conf. on Nuclear Spectroscopy and Nuclear Structure), Nauka, Moscow (1974), p. 55.
[41]O. E. Kraft *et al.*, Tezisy dokladov na XXV soveshchanii po yadernoĭ spektroskopii i strukture yadra (Abstracts of Papers at the 25th Conf. on Nuclear Spectroscopy and Nuclear Structure), Nauka, Moscow (1975), p. 63.
[42]O. E. Kraft *et al.*, Soobshchenie (Communication) R15-8810, JINR, Dubna (1975); Izv. Akad. Nauk SSSR Ser. Fiz. **39**, 1268 (1975).
[43]K. Ramavataram *et al.*, Phys. Rev. C **9**, 237 (1974).
[44]I. F. Wimpey, G. E. Mitchell, and E. G. Bilpuch, Nucl. Phys. **A9**, 9 (1974).
[45]A. A. C. Klasse and P. F. A. Goudsmit, Z. Phys. **266**, 75 (1974).
[46]M. Mazari, W. Buechner, and R. de Figueiredo, Phys. Rev. **108**, 373 (1957).
[47]Nucl. Data B **2**, No. 3 (1967).
[48]O. E. Kraft *et al.*, XXVI soveshchanie po yadernoĭ spektroskopii i strukture yadra (Proc. of the 26th Conf. on Nuclear Spectroscopy and Nuclear Structure), Nauka, Moscow (1976), p. 56; Izv. Akad. Nauk SSSR Ser. Fiz. **41**, 44 (1977).
[49]O. E. Kraft *et al.*, XXVI soveshchanie po yadernoĭ spektroskopii i strukture yadra (Proc. of the 26th Conf. on Nuclear Spectroscopy and Nuclear Structure), Nauka, Moscow (1976), p. 54.
[50]I. M. Borkin *et al.*, Izv. Akad. Nauk SSSR Ser. Fiz. **30**, 271 (1966).
[51]K. Ramavataram *et al.*, Nucl. Phys. **A191**, 88 (1972).
[52]Nucl. Data B **16**, No. 3 (1975).
[53]Yu. V. Naumov, Izv. Akad. Nauk SSSR Ser. Fiz. **39**, 1645 (1975).
[54]K. Ikeda, Prog. Theor. Phys. **31**, 434 (1964).
[55]C. Gaarde *et al.*, Nucl. Phys. **A184**, 241 (1972).
[56]J. D. Anderson, C. Wong, and V. A. Madsen, Phys. Rev. Lett. **24**, 1074 (1970).
[57]G. E. Brown and M. Bolsterli, Phys. Rev. Lett. **3**, 472 (1959).
[58]A. Goswami and M. Pal, Nucl. Phys. **35**, 544 (1962).

Translated by Julian B. Barbour